Radiation from relativistic electrons in a magnetic undulator

D. F. Alferov, Yu. A. Bashmakov, and P. A. Cherenkov

P. N. Lebedev Physics Institute, USSR Academy of Sciences
Usp. Fiz. Nauk **157**, 389–436 (March 1989)

The review sets forth the main results of theoretical and experimental studies of the radiation emitted by relativistic charged particles in undulators. The physical basis of the action of undulators is described. The main properties of undulator radiation and their relation to the trajectory of the particles in the undulator are discussed. Quantitative relations are given for the spectral, angular, and polarization characteristics of the radiation by an individual particle. The influence of the electron-beam parameters on the properties of the radiation are considered. The relation between the size of the diaphragm and the spectral characteristics of the radiation selected by it is analyzed. Some fundamental aspects and the results of recent experiments on generation of coherent undulator radiation are presented, including radiation from free electron lasers. Various types and features of undulators are described, and also characteristics of existing sources of undulator radiation in synchrotrons and storage rings. Several methods of experimental investigation and results obtained therein are discussed.

1. INTRODUCTION

As the result of the extensive possibilities of practical applications, recently methods of obtaining electromagnetic radiation from relativistic electron and positron beams are being developed intensively. The radiation emitted by high-energy electrons in external magnetic fields has a number of attractive properties: high intensity, sharp directivity, polarization, and accurately calculable spectral characteristics. Therefore steadily increasing scientific and technical uses are being found for synchrotron radiation (SR) which accompanies the motion of electrons and positrons in the bending magnets of synchrotrons and storage rings.[1-8] However, with all their desirable properties, synchrotron radiation sources cannot completely satisfy all requirements which arise on the characteristics of the radiation: intensity, spectral range, monochromaticity, and the possibility of adjustment of the form of polarization during use. Radiation which satisfies all these requirements to a significant degree can be obtained by passage of relativistic charged particles through an undulator. In an undulator electromagnetic radiation is emitted as a result of the oscillatory motion of the fast charged particles. A motion of this type is realized, for example, in a spatially periodic static magnetic field (a magnetic undulator), in crystals (natural undulators), in the field of an electromagnetic wave, and in a number of other structures. The first indication of the very promising possibilities of use of artificial periodic structures for generation of microwaves by fast particles was given many years ago in an article by V. L. Ginzburg.[9]

In the studies which followed in the fifties many attempts were made to create efficient sources of microwaves employing magnetic undulators and linear electron accelerators.[10-13] However, these ideas did not receive further development in their time in view of the difficulties of producing electron bunches with the required parameters. In addition, the lack of sources of high-energy electrons limited the possibilities of generation of more energetic photons.

At the beginning of the seventies as the result of the coming into operation of electron accelerators of intermediate energy ($E \sim 1$ GeV) the possibility appeared of a substantial increase in the energy of undulator radiation (UR). For example, in the external electron beam of the Erevan synchrotron undulator radiation was obtained in the x-ray wavelength region.[14] References 2, 15, and 16 pointed out the possibility of a significant increase of the intensity of UR as the result of use of circulating beams of ultrarelativistic electrons in synchrotrons and storage rings. This circumstance resulted in a new wave of interest in UR sources. In this period, mainly by the efforts of Soviet scientists, a comprehensive theoretical analysis of the properties of undulator radiation was carried out, which made it possible to determine the physical characteristics of UR sources which distinguish it from and provide advantages over SR. The principal results of these studies are quite completely described in several reviews.[17-21]

The first experimental studies of the properties of undulator radiation from the orbit of a cyclic accelerator, carried out in 1977–1979 in the synchrotrons Pakhra at the Lebedev Institute in Moscow[22-26] and Sirius at the Tomsk Polytechnic Institute[27-29] and subsequent work in storage rings[30-38] confirmed the main consequences of the theory and demonstrated the possibility of creating intense tunable sources of monochromatic radiation with a high degree of polarization. At the same time there has been a continuation of the intensive development and creation of new sources of undulator radiation in the very large electron storage rings which are in operation and being planned. There has been serious discussion of the need of creating a specialized storage ring with an extensive set of undulators, each of which individually is optimally planned for specific experimental problems.

An important direction of the studies, which has developed simultaneously with work on production of spontaneous undulator radiation in the energetic region of the spectrum, is the development and production of sources of coherent undulator radiation–free electron lasers (FEL). This direction has received specially intensive development after the first successful experiments on generation of induced undulator radiation in the infrared region.[39,40] In devices of this type a significant part of the energy of a well shaped electron beam can be converted directly into coherent radiation, which permits increase of the spectral density of UR in a given range by another several orders of magni-

 0038-5670/89/030200-28$01.80

tude in comparison with spontaneous radiation. In consideration of the fact that the contemporary state of the free electron laser problem has been described in rather great detail in numerous reviews,[41-51] in the present article in discussion of FEL we shall limit ourselves to consideration of some fundamental aspects and the results of recent experiments.

On the other hand, sources of spontaneous UR, which are now being used under real experimental conditions, have not been given sufficient coverage in the literature.

2. PRINCIPLES OF OPERATION OF AN UNDULATOR. QUALITATIVE DISCUSSION

2.1. Dynamics of particles in a magnetic undulator. Among various types of undulators, the most widespread are those with a magnetic field of alternating sign.[10] A schematic drawing of such an undulator and the trajectories of particles moving in it is given in Fig. 1.

An undulator consists of two periodic systems, each of which contains a large number of magnetic poles of alternating polarity. The strength of the transverse magnetic field of the undulator varies along its z axis according to a law close to sinusoidal with a period λ_0. A relativistic particle entering the undulator at a small angle α to its axis experiences the action of the undulator magnetic field, which leads to curvature of the initial trajectory of the particle.

If the initial conditions for entry of the particle into the undulator are appropriately chosen, in each oscillation the particle will cross the undulator axis each time at the same angle α_m. The value of this angle will be an important parameter in the subsequent discussion. Thus, the particle will move relative to the undulator axis in an almost sinusoidal trajectory with a period λ_0. Since the force exerted on the particle by a static magnetic field is always directed normal to its velocity and the loss of energy to radiation is negligible, the absolute value of the particle velocity, like its energy, is preserved in motion in the undulator being discussed. For constancy of the magnitude of the velocity v of the particle the lengthening of its path due to transverse oscillations with respect to the undulator axis leads to some decrease of its velocity averaged along the undulator axis $v_{\parallel} = c\beta_{\parallel}$ in comparison with its absolute value $v = c\beta$.

Therefore in an undulator a particle moves along a curved trajectory with a velocity which varies in sign and magnitude, and consequently emits electromagnetic radiation. The magnitude and orientation of the electric vector of the field of this radiation are determined by the magnitude

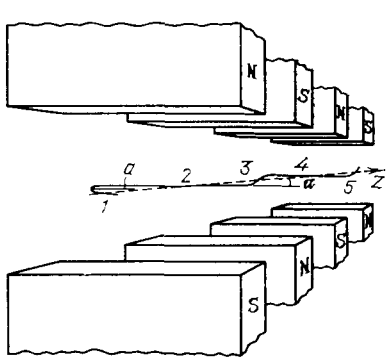

FIG. 1. Diagram showing the principle of a magnetic undulator.

and direction of the acceleration. For a periodic change of acceleration the electric field of the undulator radiation also will be a function periodic in time. We note at once that in the general case this function is not necessarily harmonic.

The trajectory of motion of a particle in an undulator will be a periodic unclosed curve. Motion along such a curve can be considered to be a bounded oscillatory motion with respect to a uniformly moving center and a translation of the center itself. The translational motion of this center can be easily excluded from the discussion by going over to a coordinate system moving uniformly along the undulator axis with the average particle velocity $v_{\parallel}$. In such a system, which in what follows we shall call the co-moving system, a particle will now execute a periodic motion along a closed trajectory. The specific form of this trajectory is determined by a number of factors, in particular by the geometry of the magnetic field and its magnitude. The radiation which arises here is undulator radiation, and we will now proceed to discuss this radiation.

2.2. Undulator radiation as radiation of a rapidly moving oscillator. An observer located in the co-moving system, as a consequence of the relativistic contraction will see the undulator magnets and the gaps between them shortened by $\gamma_{\parallel}$ times, where $\gamma_{\parallel} = (1-\beta_{\parallel}^2)^{-1/2}$ is the Lorentz factor, as a consequence of which the frequency of the oscillations of the particle, which in the laboratory system is $\Omega = 2\pi\beta_{\parallel}c/\lambda_0$, will be increased by the same factor and will be equal to

$$\omega^* = \Omega\gamma_{\parallel}. \tag{2.1}$$

Note that the field of the magnets in the co-moving system is equivalent to the field of a plane electromagnetic wave with frequency ω^*. Therefore in this system of coordinates we are dealing with the radiation of a stationary oscillator with an eigenfrequency ω^*. For an amplitude a of the harmonic oscillations of such an oscillator much smaller than the wavelength $\lambda^* = 2\pi c/\omega^*$ the radiation will have a dipole nature with a clearly expressed fundamental frequency ω^* and highly suppressed harmonics of higher multipolarities.[52] The simplest example of such a radiator is a short linear antenna–a one-dimensional dipole. A widely known example of the radiation of a two-dimensional dipole is the radiation of a nonrelativistic electron in motion in a circle in a uniform magnetic field–cyclotron radiation.[53-54] The frequency of this radiation is equal to the frequency of rotation of the electron.

If we take into account that the average velocity of the motion of the particle considered along a trajectory with a characteristic oscillation amplitude $\sim a$ and a frequency ω^* is $v \approx a\omega^*/2\pi$, we can rewrite the criterion of dipole nature of the radiation in equivalent form as a limit on the velocity $v^*/c \ll 1$; that is, the radiation will be dipole if the particle moves with a nonrelativistic velocity.

The limited time of radiation (i.e., the time of passage through the undulator) determines the natural width of the spectral line corresponding to the fundamental frequency ω^*. In the co-moving coordinate system the dipole moment **p** of a particle oscillating in an undulator is oriented normally to the velocity of this system, and the radiation is axially symmetric with respect to **p** and does not occur in the direction of this vector. In the transition to the laboratory coordinate system the direction of propagation of the radiation and

its frequency change substantially. Specifically, as a consequence of the aberration of light the radiation propagating in the co-moving system into the forward hemisphere is transformed into a narrow ray lying within a cone with opening angle $\sim 1/\gamma_{\parallel}$. For an ultrarelativistic particle, i.e., a particle whose energy $\mathscr{E}$ is much greater than the rest energy,

$$\gamma = \frac{\mathscr{E}}{mc^2} \gg 1,$$

this leads to a high directivity of the radiation. As a consequence of the Doppler effect the frequency of the radiation becomes

$$\omega(\theta) = \frac{\omega^* (1-\beta_{\parallel})^{1/2}}{1-\beta_{\parallel}\cos\theta} = \frac{\Omega}{1-\beta_{\parallel}\cos\theta}, \tag{2.2}$$

where θ is the angle formed by the direction of observation with the undulator axis z. Therefore on conversion to the laboratory system instead of one frequency of radiation ω^* we obtain a spectrum of frequencies, and to each observation angle θ there corresponds its own frequency.

If the amplitude of the oscillations of the particle is small (the criterion of smallness will be specified more accurately later), its average velocity $\beta_{\parallel}c$ will practically coincide with the total velocity βc ($\beta_{\parallel} = \beta$) and consequently $\gamma_{\parallel} = \gamma$. In addition, if we take into account that for an ultrarelativistic particle, $1-\beta \ll 1$, we can write

$$\frac{\Omega}{2} \leqslant \omega \leqslant \omega_m = 2\Omega\gamma^2; \tag{2.3}$$

we arrive at the conclusion that for a relativistic energy, with increase of the energy there is a rapid increase of the frequency of radiation from the particle.

2.3. Condition of dipole nature of undulator radiation. We shall consider the motion of a particle in an undulator along a sinusoidal trajectory with period λ_0 and amplitude a. The angle of intersection of this trajectory with the undulator axis is

$$\alpha_m = \frac{2\pi a}{\lambda_0}.$$

In what follows we shall discuss only systems with angles $\alpha_m \ll 1$, since they present the greatest practical interest. As consequence of the oscillations, the pathlength of the particle in one element of the undulator structure increases by an amount

$$\frac{1}{4}\left(\frac{2\pi a}{\lambda_0}\right)^2 \lambda_0 = \frac{1}{4}\alpha_m^2\lambda_0.$$

This quantity is important, since it determines the slowing down of the velocity of longitudinal motion of the particles,

$$\beta_{\parallel} = \beta\left(1 - \frac{1}{4}\alpha_m^2\right), \tag{2.4}$$

and the corresponding decrease of the longitudinal Lorentz factor $\gamma_{\parallel}$ to a value

$$\gamma_{\parallel} = (1-\beta_{\parallel}^2)^{-1/2} = \gamma\left[1 + \frac{1}{2}(\alpha_m\gamma)^2\right]^{-1/2} \tag{2.5}$$

Equation (2.5) has great significance as a result of the fact that this equation, and not Eq. (2.4), determines the conditions under which it is possible to neglect the change of the average velocity of longitudinal motion of a particle[55]

$$\alpha_m\gamma \ll 1. \tag{2.6}$$

As will be shown below, the condition (2.6) is simultaneously the condition of dipole nature of the radiation in the co-moving coordinate system. However, it is important to note that a change of the velocity of longitudinal motion leads to a further very important effect–the appearance of oscillations of the particle along the undulator axis (trembling). In fact, at the peaks of the sinusoidal trajectory the particle velocity is directed along the undulator axis z and exceeds $\beta_{\parallel}c$ (2.4), while at the intersections of the trajectories with the undulator axis the projection of the velocity on the z axis $\beta_z c = \beta c[1 - (1/2)\alpha_m^2]$ is less than the average longitudinal velocity. As has been shown in Refs. 17 and 55–57, the contribution of these oscillations to formation of the radiation spectrum turns out to be extremely significant in spite of their small amplitude

$$\delta z_m \approx \frac{\lambda_0}{2}\frac{\delta\beta_z}{\beta} = \frac{\alpha_m a}{8\beta}.$$

It is of interest to analyze these oscillatory motions in the co-moving system. Lorentz transformations show that in the absence of trembling the motion in this system would be uniform. Radiation in such motions has been discussed in Refs. 58–60. On the other hand, the existence of trembling has the result that the motion becomes two-dimensional. The complete trajectory has the characteristic form of a figure eight (Fig. 2) oriented along the x' axis. The maximum deviation from the z' axis is $x'_m = a$, and the displacement along this axis due to trembling is $z'_m = \alpha_m\gamma_{\parallel}a$. As can be seen, these quantities are comparable if $\alpha_m\gamma \approx 1$. For $\alpha_m \ll 1$ the figure eight degenerates into a straight-line segment—the dipole approximation.

The expression for the velocity of motion of the particle in the co-moving system with inclusion of trembling takes the form[61]

$$v'^2 = c^2\left[1 - \frac{4(1-2b^2)}{(2+2b^2-k_0^2x'^2)^2}\right], \tag{2.7}$$

where

$$b^2 = \frac{\alpha_m^2\gamma_{\parallel}^2}{4} = \frac{\alpha_m^2\gamma^2}{4[1+(1/2)\alpha_m^2\gamma^2]}, \quad k_0 = \frac{\Omega\gamma_{\parallel}}{c},$$

$$k_0x'_m = k_0a = \alpha_m\gamma = 2(b^2)^{1/2}.$$

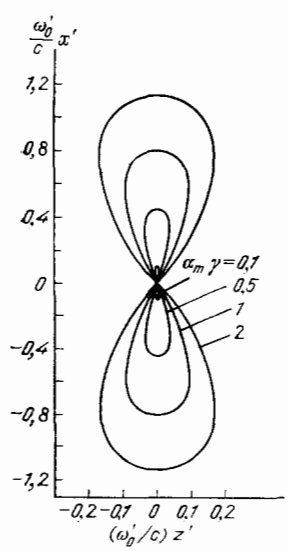

FIG. 2. Trajectory of particle in the co-moving system S'.

The velocity of the particle in its motion along the figure eight varies: the longitudinal velocity is greatest at the tips of the figure eight ($|x'| = a$):

$$v'_{zm} = \frac{c\alpha_m^2\gamma^2}{4+\alpha_m^2\gamma^2},$$

and the total velocity is greatest on crossing the origin of the coordinates ($x' = 0$):

$$v'_m = c\alpha_m\gamma\frac{(16+9\alpha_m^2\gamma^2)^{1/2}}{4+3\alpha_m^2\gamma^2}.$$

The energy of the particle in the laboratory coordinate system $\mathscr{E} = (\mathscr{E}' + v_\parallel p'_z)\gamma_\parallel$ (p'_z is the component of the momentum) in the absence of trembling ($p'_z = 0$) is proportional to the energy $\mathscr{E}'$ in the co-moving coordinate system. In view of conservation of the energy $\mathscr{E}$ the variation of $\mathscr{E}'$, which is substantial in the nondipole case, unavoidably leads to the appearance of p'_z.

2.4. Interference phenomena in an undulator. The time T of passage of a particle through an undulator (and consequently the time of emission by it of electromagnetic radiation) is $L/\beta_\parallel c$, where $L = K\lambda_0$ is the length of an undulator consisting of K elements of periodicity. The duration of the pulse of radiation in the direction θ (Fig. 3) is determined by the difference between the velocity of light and the projection of the velocity of the particle on the direction of observation. In a time T the radiation emitted at the beginning of the undulator will traverse a distance

$$l = cT = \frac{L}{\beta_\parallel}.$$

The projection of the final point of the undulator on the direction of propagation of the radiation is removed from the beginning of the undulator by a distance $L\cos\theta$. Thus, the length of the train of undulator radiation is

$$\Delta l = l - L\cos\theta = \frac{L}{\beta_\parallel}(1-\beta^\parallel\cos\theta).$$

K complete oscillations fit into a length Δl, and consequently the length of the wave which is dominant in the radiation (the length of one oscillation) is

$$\lambda = \lambda_0(1-\beta_\parallel\cos\theta)\beta_\parallel^{-1}.$$

The greatest contribution to the intensity of all waves emitted in a given direction will be given by those waves λ_m which in the entire length of the undulator are in identical phase with respect to the particle moving in it. Then the amplitudes of these waves in their motion through the undulator will continuously rise. For wavelengths λ different from λ_m, the wave will acquire a phase advance $\Delta\varphi$ relative to the particle, and this phase advance will accumulate faster, the larger is $\Delta\lambda = \lambda - \lambda_m$. The radiation from those points of the undulator for which this advance is $\Delta\varphi = \pi$ will mutually cancel.

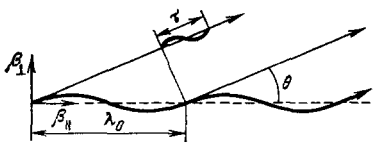

FIG. 3. Formation of a pulse of radiation in an undulator.

Let us find the condition of synchronism of a wave of frequency ω propagating at an angle θ to the undulator axis and a particle executing in the undulator periodic oscillations with respect to its axis with frequency Ω. For this purpose it is necessary that the increment in some time interval Δt of the phases of the electron oscillations and of the oscillations of the waves be equal. During this time the phase of the electron oscillations changes by $\Omega\Delta t$, and the electron itself is displaced along the undulator axis by $\Delta z = \beta_\parallel c\Delta t$. With this displacement the phase of the electromagnetic wave changes by a value $\omega\Delta t - (\omega/c)\cos\theta\Delta z$. Equating the phase changes obtained, we find the condition of synchronism of the wave and the particle: $\Omega = \omega(1-\beta_\parallel\cos\theta)$. The detuning of the wave frequency $\Delta\omega$ at which the phase advance in the entire length of the undulator will amount to a value π, with allowance for the fact that $\Delta t = K\lambda_0/\beta_\parallel c$, will be

$$\Delta\omega = \pi[(1-\beta_\parallel\cos\theta)\Delta t]^{-1}.$$

Hence, using Eq. (2.2), we obtain

$$\frac{\Delta\omega}{\omega} = \frac{1}{2K}.$$

This relation also characterizes in order of magnitude the width of the spectral line of the undulator radiation observed at a given angle θ.

3. PARTICLE TRAJECTORIES IN UNDULATORS

The nature of the oscillatory motion of a particle is given by the form of the undulator magnetic field and, in the general case, can turn out to be extremely complex. However, in most cases of practical interest the motion of the particle can reduce to the two simplest forms: sinusoidal and motion along a helical trajectory.

3.1. Motion of charged particles in a planar undulator. In a planar magnetic undulator there is formed a transverse magnetic field whose intensity vector is perpendicular to the median plane of the undulator (see Fig. 1) and varies along the z axis according to a harmonic law

$$\mathbf{H} = -\mathbf{j}H_m\sin\frac{2\pi}{\lambda_0}z \quad (0\leqslant z\leqslant L), \tag{3.1}$$

where $\mathbf{j}$ is a unit vector along the y axis, perpendicular to the undulator z axis (in what follows we shall everywhere take the undulator axis as the z axis of the coordinate system), and H_m is the amplitude of the magnetic field. The trajectory of an electron in such an undulator will lie in the x,z plane and for the condition $\alpha_m \ll 1$, where $\alpha_m = eH_m\lambda_0/2\pi mc^2\gamma$, is given by the expression[10,17,55,56,62]

$$\mathbf{r}(t) = \mathbf{i}x_m\sin\Omega t + \mathbf{k}[c\beta_\parallel t - (\delta z)_m\sin 2\Omega t], \tag{3.2}$$

where $x_m = c\alpha_m/\Omega$ and $\Omega = 2\pi\beta_\parallel c/\lambda_0$ are the amplitude and frequency of the transverse oscillations, respectively, $(\delta z)_m = \Omega x_m^2/8\beta c$ is the amplitude of the longitudinal oscillations, which occur with a doubled frequency 2Ω (trembling), and

$$c\beta_\parallel = c\beta\left(1-\frac{\alpha_m^2}{4\beta^2}\right)$$

is the average velocity along the undulator axis. The equation of motion (3.2) is valid for initial conditions at $t = 0$ at the entrance to the undulator selected specially:

$$x=y=z=0, \quad \frac{dx_m}{dt}=\alpha_m c.$$

It follows from it that in the relativistic case ($\beta_{\parallel} \sim 1$) the frequency of oscillations depends only weakly on the particle energy, while the amplitude of the oscillations depends on the field amplitude H_m and the period λ_0 and decreases rapidly with increase of the energy. For other initial conditions a slow transverse drift of the particles will occur. In a sufficiently long undulator in view of the inhomogeneity of the magnetic field the drift will go over into slow oscillations of the particles about the undulator axis.

As was pointed out previously (Chap. 2), an important characteristic of an undulator is the dimensionless quantity

$$\alpha_m \gamma = \frac{eH_m \lambda_0}{2\pi mc^2}, \tag{3.3}$$

which determines the form of the spectrum of undulator radiation. Using Eq. (3.3), we can represent the condition of dipole nature of the radiation (2.6) in the form

$$H_m \lambda_0 \ll \frac{2\pi mc^2}{e}. \tag{3.4}$$

For electrons and positrons this formula becomes $H_m \lambda_0 \ll 10700$ Oe·cm. For particles heavier than an electron the quantity on the right increases in proportion to the mass of these particles. For example, for protons we obtain the following condition: $H_m \lambda_0 \ll 19.6 \cdot 10^6$ Oe·cm, which is practically always satisfied.

It is interesting to note that the relations

$$\Omega t = \frac{2\pi}{\lambda_0} \beta_{\parallel} ct \approx \frac{2\pi}{\lambda_0} z(t)$$

provide the possibility of representing the field at each point of the particle trajectory as a linear function of its transverse displacement x:

$$\mathbf{H} \approx -\mathbf{j} \frac{H_m}{x_m} x \quad (x \leqslant x_m)^{63}.$$

This same dependence of the field on the transverse displacement is characteristic also of systems with a quadrupole electric or magnetic field of the form

$$\mathbf{H} = \mathbf{j} g x \tag{3.5}$$

(g is the field gradient), which can be used as an undulator.[64,65] A field of the form (3.5) is produced in the quadrupole lenses which are used for formation and control of charged-particle beams.[67] The trajectory of a particle moving in the lens is determined by the same formula (3.2). However, in this case the main parameters of the trajectory are determined by the initial conditions. For example, the oscillation amplitude x_m and the angle α_m are determined by the coordinate and the angle of entry of the particle into such an undulator. The frequency of harmonic oscillations

$$\Omega = \left(\frac{eg}{m\gamma}\right)^{1/2} \tag{3.6}$$

is not only determined by the field gradient, but also depends on the particle energy.[64,67] With increase of the particle energy the oscillation frequency decreases as $\gamma^{-1/2}$, and the oscillation period in turn increases as $\gamma^{1/2}$. Therefore the condition of dipole radiation (2.6) should be rewritten as a limit on the oscillation amplitude[64]

$$x_m \ll \left(\frac{mc^2}{eg\gamma}\right)^{1/2}. \tag{3.7}$$

If the lens aperture remains constant an increase of the particle energy can lead to destruction of the dipole nature of the radiation. For such an undulator of fixed length the number of its periods drops with increase of the energy as $\gamma^{-1/2}$.

For macroscopic quadrupole lenses the gradients achievable in practice turn out to be extremely small, which leads to large oscillation periods (of the order of a meter). Crystals are another matter—they can be regarded as special natural undulators.[63] In the channels formed by the crystal planes there is a transverse electric field,[68] which varies according to a law $\mathbf{E} \approx \mathbf{i} g x$, and the gradients are extremely large. The trajectory of a charged particle in such channels is described by Eq. (3.2). The periods of their oscillations may amount to thousands or tens of thousands of angstroms (10^{-5}–10^{-4} cm). Therefore the radiation from channeled particles has recently been attracting the close attention of physicists as a possible source of energetic quasimonochromatic radiation.[69–74]

3.2. Motion of charged particles in a helical undulator. As has been shown in several papers,[17,75,76] the magnetic field near the axis of a helical undulator varies according to a law

$$\mathbf{H} = \mathbf{i} H_m \sin \frac{2\pi}{\lambda_0} z \mp \mathbf{j} H_m \cos \frac{2\pi}{\lambda_0} z \quad (0 \leqslant z \leqslant L), \tag{3.8}$$

where H_m is the magnetic field strength, which remains constant over the entire length of the undulator.

With displacement along the undulator axis the end of the magnetic field vector laid out from this axis describes a helical line which is right-handed or left-handed depending on the sign (−) or (+) in front of the second term in Eq. (3.8). In such a field for the initial conditions

$$y=z=0, \quad x=R, \quad \frac{dx}{dt}=0, \quad \frac{dy}{dt}=\pm \alpha_m c, \quad t=0$$

the particle moves along a helix determined by the expression

$$\mathbf{r}(t) = \mathbf{i} R \cos \Omega t \pm \mathbf{j} R \sin \Omega t + \mathbf{k} \beta_{\parallel} ct, \tag{3.9}$$

where $R = \alpha_m c/\Omega$ is the radius of the helix and $\alpha_m = eH_m \lambda_0 / 2\pi mc^2 \gamma$ is the angle of winding of the helix. Motion along the z axis occurs with a constant velocity

$$\beta_{\parallel} c = \beta c \left(1 - \frac{\alpha_m^2}{2\beta^2}\right),$$

and here again the condition $\alpha_m \ll 1$ is assumed to be satisfied. Note that as a result of the difference in the geometry of the magnetic field the expression for the longitudinal velocity of a particle in a helical undulator differs by a factor of two in front of α_m^2 from the corresponding expression for a planar undulator. In the co-moving coordinate system the motion of the particles in a helical undulator is represented as motion in a circle of radius R, whose plane is oriented normal to the undulator axis. Trajectories of this type are followed by particles emitted into a uniform magnetic field at a small angle to the direction of the magnetic line of force. However, here also, as in a quadrupole field, the undulator period increases with increase of the energy, whereas in a helical undulator it is given by the winding step of the helix. A motion close in nature to the motion along a helix occurs also in axial channeling of particles in crystals.[70–74]

We note that according to Refs. 17, 61, and 77–79 a motion of relativistic charged particles according to laws of

motion close to (3.2) and (3.9) occurs also in the field of an intense electromagnetic wave with linear or circular polarization, which can be discussed as one type of undulator. However, with the intensities I_b achievable at the present time, the field strength of such an undulator, which is given by $E(\mathrm{V/cm}) \approx 20\, I_b\ \mathrm{W/cm^2})^{1/2}$, is quite inferior to that of a magnetic undulator.

In addition to the harmonic (ideal[15,64]) undulators discussed above, anharmonic undulators also exist in nature.[17] For example, the transverse motion of charged particles in crystals is characterized in a number of cases by strong anharmonicity.[17] An example is the motion of electrons relative to a crystallographic plane (or axis) whose potential can be described by means of an inverted parabola, in contrast to positrons, for which the potential is represented by an ordinary parabola.[80] As is well known from the theory of accelerators,[67,81] in each individual parabolic portion of the potential, the transverse motion of positrons can be described bv trigonometric functions, and that of electrons by hyperbolic functions.[69,82]

4. QUANTITATIVE CHARACTERISTICS OF UNDULATOR RADIATION

4.1. General properties of undulator radiation. The discussion of undulator radiation in most cases of practical interest is carried out in the framework of classical electrodynamics. The electric field **E** and the magnetic field **H** of a charge at time t at a point of observation given by a radius vector $\mathbf{R}(t) = R\mathbf{n}$ ($\mathbf{n}$ is a unit vector) measured from the charge are determined by the motion of the charge at a previous moment of time t' from the Lienard-Wiechert potentials[52,54]

$$\mathbf{E} = e\frac{1-\beta^2}{R^2(1-\mathbf{n}\boldsymbol{\beta})^3}(\mathbf{n}-\boldsymbol{\beta}) + \frac{e}{cR(1-\mathbf{n}\boldsymbol{\beta})^3}[\mathbf{n}[(\mathbf{n}-\boldsymbol{\beta})\dot{\boldsymbol{\beta}}]], \quad (4.1)$$

$$\mathbf{H} = [\mathbf{n}\mathbf{E}]. \quad (4.2)$$

Here the square brackets indicate a vector product, all quantities on the right-hand side are taken at the moment of time $t'(t' + R(t')c^{-1} = t)$, and $\dot{\boldsymbol{\beta}} = \partial\boldsymbol{\beta}/\partial t'$. The electromagnetic radiation is determined by the second term in Eq. (4.1), which depends on the acceleration.

According to Eq. (4.1) the radiation of an ultrarelativistic particle is concentrated mainly along the instantaneous direction of its velocity in a region of angles $\sim 1/\gamma$, since just for these directions the quantity $(1-\mathbf{n}\cdot\boldsymbol{\beta})^3$ in the denominator of (4.1) takes its minimum value $\sim(1-\beta)^3$. For vectors **n** lying in the plane of motion $\boldsymbol{\beta}\cdot\dot{\boldsymbol{\beta}}$ and forming with the velocity an angle $\psi = \arccos\beta \approx \gamma^{-1}$, the radiation field vanishes.

On the axis of a planar undulator (see Eq. (3.2)) the radiation term in (4.1) gives

$$E_{x,\mathrm{rad}} \approx \frac{8\pi e(\alpha_m\gamma)\gamma^3}{R\lambda_0}.$$

The "Coulomb" term along the x axis also gives a variable field shifted in phase relative to the radiative term by a half-period of the oscillations, $E_{x,\mathrm{Coul}} \approx 8e(\alpha_m\gamma)\gamma^3/R^2$. These quantities are close in order only within the undulator, when $R \sim \lambda_0$. The constant longitudinal field is $E_{z,\mathrm{Coul}} \approx 4e\gamma^2/R^2$ and for $\gamma \gg 1$, $R \gtrsim \lambda_0$, it is much less than the two terms discussed. In what follows we shall be interested in the radiation far from the undulator and therefore we shall not consider the first term in (4.1).

Far from the undulator in the wave zone, where $R \gg L$, the variation of **R** and **n** in (4.1) can be neglected in motion of a particle in an undulator. The spectral and angular distribution of the radiation energy at frequency ω in the direction determined by the vector **n**, in the wave zone where the waves in small regions of space can be considered plane, are given by the expression[52,54]

$$\frac{d^2\mathscr{E}}{d\omega\, do} = \frac{c}{4\pi^2}|\vec{\mathscr{E}}_\omega|^2 R_0^2 = \frac{e^2}{4\pi^2 c}|\mathbf{A}_\omega|^2, \quad \vec{\mathscr{E}}_\omega = \frac{e}{R_0 c}\mathbf{A}_\omega,$$

$$\mathbf{A}_\omega = \int_{-\infty}^{+\infty}[\mathbf{n}[(\mathbf{n}-\boldsymbol{\beta})\dot{\boldsymbol{\beta}}]](1-\mathbf{n}\boldsymbol{\beta})^{-2}\exp\left[i\omega\left(t-\frac{\mathbf{n}\mathbf{r}(t)}{c}\right)\right]dt, \quad (4.3)$$

where $d\mathscr{E}$ is the energy radiated by a particle into an element of solid angle do in the frequency interval $d\omega$, R_0 is the radius vector drawn from the beginning of the undulator to the point of observation, $\mathbf{R}(t) = \mathbf{R}_0 - \mathbf{r}(t)$, and $\mathbf{r}(t)$ is the radius vector of the particle measured from the beginning of the undulator (see Chap. 3). The radiation spectrum of the particle is formed in accordance with Eq. (4.3) on the entire trajectory of the particle.

We note that from (4.3) it is possible to eliminate acceleration if one makes use of the equality

$$\frac{[\mathbf{n}[(\mathbf{n}-\boldsymbol{\beta})\dot{\boldsymbol{\beta}}]]}{(1-\mathbf{n}\boldsymbol{\beta})^2} = \frac{d}{dt}\frac{[\mathbf{n}[\mathbf{n}\boldsymbol{\beta}]]}{1-\mathbf{n}\boldsymbol{\beta}}$$

and carries out integration by parts.

In the general case the spectral and angular distribution of the energy of the radiation in an undulator with a large number of elements of periodicity $K \gg 1$ can be represented in the form of the sum of the radiations of the individual harmonics[17,57]

$$\frac{d^2\mathscr{E}}{d\omega\, do} = \frac{e^2}{\pi^2 c}\sum_{k=1}^{\infty}\frac{|\mathbf{a}_k(\omega,\theta,\varphi)|^2}{\Omega^2}\frac{\sin^2(\pi K\sigma_k)}{\sigma_k^2}, \quad (4.4)$$

where the vector $\mathbf{a}_k$ is given by

$$\mathbf{a}_k = \frac{\Omega}{2\pi}\int_0^{2\pi/\Omega}\mathbf{a}(t)e^{i\Omega t}dt,$$

$$a(t) = [\mathbf{n}[(\mathbf{n}-\dot{\boldsymbol{\beta}})\boldsymbol{\beta}]](1-\mathbf{n}\boldsymbol{\beta})^{-2}\exp\left[-\frac{i\omega}{c}(n_x x + n_y y + n_z\delta z)\right],$$

$$\sigma_k(\omega,\theta) = \Omega^{-1}[\omega(1-n_z\beta_{\|}) - k\Omega],$$

$n_x = \sin\theta\cdot\cos\varphi$, $n_y = \sin\theta\cdot\sin\varphi$, $n_z = \cos\theta$, θ is the polar angle formed by **n** with the undulator axis z, and φ is the aximuthal angle formed by the projection of **n** on the x,y plane with the x axis. The vector $\mathbf{a}_k(\omega,\theta,\varphi)$ determines the dependence of the radiation characteristics on the shape and transverse dimensions of the particle trajectory in one period of its oscillations. The expression $|\mathbf{a}_k(\omega,\theta,\varphi)|^2$ in comparison with the factor $\sin^2(\pi K\sigma_k)/\sigma_k^2$ changes significantly more smoothly. Therefore the spectral and angular behavior of the radiation are determined mainly by the expression $\sin^2(\pi K\sigma_k)/\sigma_k^2$, whose dependence on σ_k is shown in Fig. 4. Its main maximum lies at $\sigma_k = 0$. It determines the frequency of the radiation of the k-th harmonic propagated at an angle θ to the undulator axis [see Eq. (2.2)].

For ultrarelativistic motion,

$$1 - n_z\beta_{\|} = 1 - \beta_{\|}\cos\theta \approx \frac{1}{2\gamma^2}\left(1 + \frac{p_\perp^2}{2} + \theta^2\gamma^2\right).$$

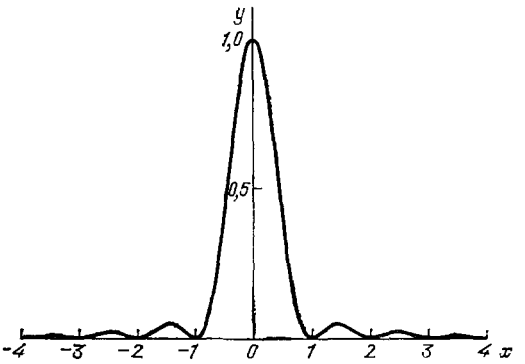

FIG. 4. Spectral and angular distribution of radiation energy in an ideal undulator.

we can rewrite the radiation frequency ω_k in the form

$$\omega_k = \frac{2k\Omega\gamma^2}{1+(p_\perp^2/2)+\theta^2\gamma^2} \quad (\theta \ll 1,\ \gamma \gg 1). \tag{4.5}$$

The frequency of radiation of a given harmonic reaches a maximum at zero angle:

$$\omega_{km} = \frac{2k\Omega\gamma^2}{1+(p_\perp^2/2)}; \tag{4.6}$$

Here $p_\perp^2/2$ is the average value of the square of the reduced transverse momentum of the particle. For a planar undulator it is given by [see Eq. (3.3)]

$$\frac{\alpha_m^2\gamma^2}{2} = \frac{1}{2}\left(\frac{eH_m\lambda_0}{2\pi mc^2}\right)^2,$$

and for a helical undulator [see Eq. (3.9)] it is given by

$$\alpha_m^2\gamma^2 = \left(\frac{eH_m\lambda_0}{2\pi mc^2}\right)^2.$$

We note that in channeling of particles in a crystal the parameter

$$p_\perp = \left(\frac{2eU_0\gamma}{mc^2}\right)^{1/2}$$

increases with increase of the particle energy; here $U_0 \approx gd^2/2$ is the interplanar potential and d is the channel width [see Eq. (3.5)].

The height of the principal maximum in Fig. 4 increases in proportion to K^2 with increase of the number of periodicity elements of the undulator. Just for this reason in a number of studies[83,84] undulator radiation is still called coherent or interference synchrotron radiation. Here one is considering the well known analogy with coherent bremsstrahlung in crystals, where periodic motion of charged particles also takes place.[85]

The first minimum $\sigma_{k_1} = 1/K$ determines the width $\Delta\omega_k$ of the spectral lines of the radiation observed at a given angle θ,

$$\Delta\omega_k = \frac{\omega_k}{kK}, \tag{4.7}$$

which falls off inversely proportional to K. According to (4.5), the radiation with a fixed frequency ω, if $\omega \lesssim \omega_{km}$, is concentrated on the surface of a cone with opening angle

$$\theta_k = \gamma^{-1}\left[\left(\frac{\omega_{km}}{\omega}-1\right)\left(1+\frac{p_\perp^2}{2}\right)\right]^{1/2}. \tag{4.8}$$

The width of the angular distribution $\Delta\theta_k$ also is found from the condition $\sigma_{k_1} = 1/K$, with $\omega = \text{const}$:

$$\Delta\theta_k = \left[\theta_k^2 + \frac{\theta_k^2}{kK} + (\Delta\theta_{k0})^2\right]^{1/2} - \theta_k, \tag{4.9}$$

where

$$\Delta\theta_{k0} = \gamma^{-1}\left[\frac{1+(p_\perp^2/2)}{kK}\right]^{1/2} \tag{4.10}$$

is the interval of angles in which is concentrated the radiation of frequency ω_{km} propagated along the undulator axis.[18] We note that for low frequencies $\omega/\omega_{km} \ll 1$, according to (4.8), the opening angle of the cone of radiation $\theta_k = (2k\Omega/\omega)^{1/2}$ does not depend on the energy of the particle.

The height of the auxiliary maxima falls off rapidly; for example, the height of the first auxiliary maximum is about 0.05 of the height of the principal maximum.

Figure 4 recalls the distribution of the intensity of radiation diffracted in a slit or opening. One can define the effective diffraction size of the radiator in an undulator as ($\theta = 0$)

$$d_k = \frac{\lambda_0}{2\gamma}\left\{\left[1+\left(\frac{p_\perp^2}{2}\right)\right]Kk^{-1}\right\}^{1/2}. \tag{4.11}$$

For $K \gg 1$ it substantially exceeds the amplitude of oscillations of the particles in the undulator x_m.

The total radiation energy in the line, determined by the area of the curve in Fig. 4, is proportional to K.

The spectral distribution of the radiation can be obtained by integration of (4.3) or (4.6) over angle, and the angular distribution can be obtained by integration of the same expressions over the frequency of radiation or by integration over time of the expression $\sim \mathbf{E}^2$, where $\mathbf{E}(t)$ is taken from (4.1).

4.2. Dipole undulator radiation. In the ultrarelativistic case in the dipole approximation [see Eq. (2.7)] in (4.3) the velocity of the charge can be considered constant and directed everywhere along the axis of the undulator. Then $\mathbf{A}_\omega$ reduces to the form

$$\mathbf{A}_\omega = \frac{[\mathbf{n}\,[(\mathbf{n}-\boldsymbol{\beta})\,\dot{\boldsymbol{\beta}}_{\omega'}]]}{(1-\mathbf{n}\boldsymbol{\beta})^2}, \tag{4.12}$$

where

$$\dot{\boldsymbol{\beta}}_{\omega'} = \int_{-\infty}^{\infty} \dot{\boldsymbol{\beta}}(t)\, e^{i\omega' t}\, dt$$

is the Fourier component of the particle acceleration and $\omega' = \omega(1-\mathbf{n}\boldsymbol{\beta}) = \omega(1-\beta\cos\theta)$.

In the co-moving coordinate system ($\beta \ll 1$) the quantity $\mathbf{A}_\omega$ is simplified still more:

$$\mathbf{A}_{\omega^*} = [\mathbf{n}^*\,[\mathbf{n}^*\dot{\boldsymbol{\beta}}_{\omega^*}]]; \tag{4.13}$$

Here $\mathbf{A}_{\omega^*}$ is the Fourier component of the acceleration normal to $\mathbf{n}^*$, and $\omega^* = \Omega\gamma$; see Eq. (2.1).

The radiation spectrum for a long undulator ($K \gg 1$) can be obtained directly from (4.4), where

$$\mathbf{a}_k = \frac{[\mathbf{n}\,[(\mathbf{n}-\boldsymbol{\beta})\,\dot{\boldsymbol{\beta}}_k]]}{(1-\mathbf{n}\boldsymbol{\beta})^2}, \qquad \dot{\boldsymbol{\beta}}_k = \frac{\Omega}{2\pi}\int_0^{2\pi/\Omega} \dot{\boldsymbol{\beta}} e^{ik\Omega t}\, dt,$$

$$\sigma_k = \Omega^{-1}(\omega' - k\Omega).$$

Integrating over angles and introducing the new variable $\xi = \omega/2\Omega\gamma^2$, we have

$$\frac{d\mathscr{E}}{d\xi}=\frac{8e^2\gamma^4}{c\Omega}$$

$$\times\sum_{k=E(\xi+1)}^{\infty}\int_1^{\infty}|\dot{\beta}_k|^2\frac{\sin^2[\pi K(u\xi-k)]}{(u\xi-k)^2}\frac{1}{u^2}\left(1-\frac{2}{u}+\frac{2}{u^2}\right)du; \tag{4.14}$$

here $E(\varkappa)$ is the integer part of the number $\varkappa$. For a very long undulator ($K\to\infty$) we can use the limiting transition

$$\lim_{K\to\infty}\frac{\sin^2[\pi K(u\xi-k)]}{\pi^3K(u\xi-k)^2}=\frac{1}{\xi}\delta(u-k).$$

As a result we obtain instead of (4.14)

$$\frac{d\mathscr{E}}{d\xi}=\frac{8\pi^3e^2K\gamma^4}{c\Omega}\sum_{k=E(\xi+1)}^{\infty}|\dot{\beta}_k|^2\frac{\xi}{k^2}\left(1-2\frac{\xi}{k}+2\frac{\xi^2}{k^2}\right). \tag{4.15}$$

The spectrum of radiation of the k-th harmonic is cut off at a frequency $\omega_{km}=2k\Omega\gamma^2$.

The higher harmonics of the radiation which arise in the dipole approximation as a consequence of the anharmonicity of the motion have, for an identical directivity of the vectors $\dot{\beta}_k$, angular distributions which are identical with the fundamental frequency, and their spectral distributions differ only in the frequency scale.

The spectral distribution of the radiation for a finite undulator with harmonic motion (planar or helical) is shown in Fig. 5. We have also shown in this figure spectra for an undulator of infinite length. The areas under the curves have been normalized to unity. In undulators of finite length the radiation extends to higher frequencies in comparison with ω_m, and the maximum of the spectrum shifts to frequencies smaller than ω_m. For sufficiently long undulators $K\gtrsim 10$ the shape of the integrated spectrum does not differ too greatly from the spectrum of an infinite undulator.[15]

4.3. Radiation in a planar undulator. The radiation in a planar undulator is symmetric with respect to the plane of motion determined by the vector $\boldsymbol{\beta}\times\dot{\boldsymbol{\beta}}\simeq\mathbf{H}$ (the horizontal plane xz; see Chap. 3). The periodic variation of the vector $\mathbf{H}$ equalizes in importance the two normals to the plane of motion. Therefore the radiation is symmetric also with respect to the vertical plane y,z passing through the undulator axis.

In a planar undulator the radiation of the particle is completely linearly polarized, and the orientation of the electric-field vector in some chosen direction of observation is given by the vector $\mathbf{a}_k$ in (4.4) and consequently will depend on this direction.

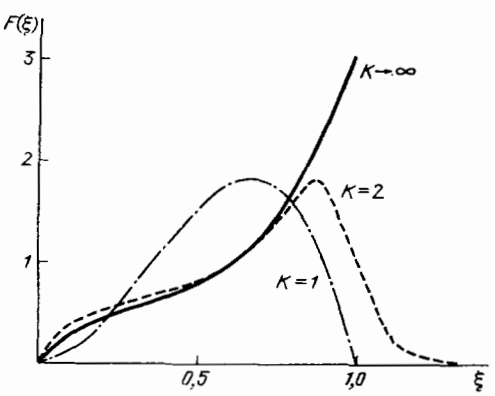

FIG. 5. Spectral distribution of radiation energy in an ideal undulator in the dipole approximation.

In the dipole approximation only one harmonic is studied, since only $\mathbf{a}_1$ is different from zero,

$$\mathbf{a}_1=\frac{i\Omega\gamma p_\perp}{1+\vartheta^2}\left[\mathbf{i}\left(1-\frac{2\vartheta^2\cos^2\varphi}{1+\vartheta^2}\right)-\mathbf{j}\frac{\vartheta^2\sin^2\varphi}{1+\vartheta^2}\right]; \tag{4.16}$$

here $\vartheta=\theta\gamma$. Along the undulator axis (with $\vartheta=0$) there is emitted only radiation whose electric-field vector is parallel to the plane of oscillations of the particles in the undulator. The maximum of the intensity of this component of the radiation for an arbitrary angle ϑ is reached in the vertical plane ($\varphi=\pi/2,\ 3\pi/2$). The intensity of radiation with electric vector perpendicular to the plane of the oscillations has four maxima at

$$\varphi=\frac{(2k+1)}{4}\pi\quad(k=0,\ 1,\ 2,\ 3).$$

For values

$$\varphi=\frac{k}{2}\pi$$

it vanishes.

The spectral and angular distribution of the radiation, summed over polarizations, is obtained after substituting (4.16) into (4.4),

$$\frac{d^2\mathscr{E}}{d\omega\,do}=\frac{8e^2p_\perp^2\gamma^2}{\pi^2\lambda_0^2c}$$

$$\times\frac{1}{(1+\vartheta^2)^2}\left[1-\frac{4\vartheta^2\cos^2\varphi}{(1+\vartheta^2)^2}\right]\frac{\sin^2\{\pi K[(\omega/\omega_1)-1]\}}{[(\omega/\omega_1)-1]^2}, \tag{4.17}$$

where

$$\omega_1=\frac{2\Omega\gamma^2}{1+\vartheta^2}.$$

In this distribution a second azimuthal harmonic appears explicitly, and in the x,z plane the energy of the radiation drops to zero at $\vartheta=1$. Similar symmetry properties are characteristic for the distribution of the instantaneous intensity of any magnetic bremsstrahlung radiation.[52] At large angles ($\vartheta\gg 1$) the itensity falls off as ϑ^{-4}.

The spectral distribution of the radiation is described by the first term ($k=1$) in (4.15).

With increase of the field in the undulator, higher harmonics also become appreciable in addition to the fundamental harmonic of the radiation. The angular and spectral distributions of even and odd harmonics differ substantially.[17,21,56,57,86,87] For example, along the undulator axis only odd harmonics ($k=2p+1$) are emitted, and their spectral and angular distribution at the maximum[17,57] of the line ($\omega=\omega_{(2p+1),m},\vartheta=0$) is

$$\frac{d^2\mathscr{E}_{2p+1}}{d\omega\,do}=\frac{K^2e^2\gamma^2}{c}F_{2p+1}(p_\perp),$$

$$F_{2p+1}(p_\perp)=\frac{(2p+1)^2p_\perp^2}{[1+(p_\perp^2/2)]^2}$$

$$\times[J_p((2p+1)\varkappa)-J_{p+1}((2p+1)\varkappa)]^2, \tag{4.18}$$

where J_p is the Bessel function of order p and

$$\varkappa=\frac{p_\perp^2}{4[1+(p_\perp^2/2)]}.$$

The dependence on the reduced transverse momentum $p_\perp$ ($p_\perp$ from 0 to 5) of the spectral and angular distribution of

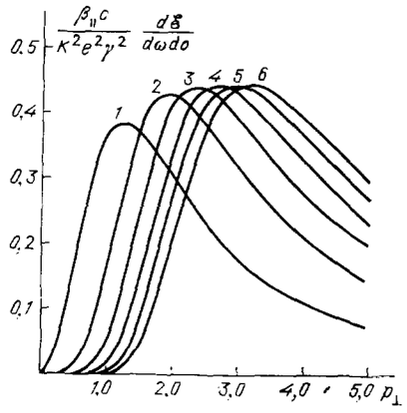

FIG. 6. Spectral and angular density of radiation in harmonics as a function of $p_\perp$ for $\theta = 0$, $2p + 1 = 1$ (curve 1), 3 (curve 2), 5 (curve 3), 7 (curve 4), 9 (curve 5), and 11 (curve 6).

the energy of the radiation at zero angle, plotted for the first few harmonics in accordance with Eq. (4.18), is shown in Fig. 6.[87] The energy of the radiation at the maximum of the line in the first harmonic first rises as the square of the magnetic field strength, after which the rate of rise slows down and it reaches a maximum

$$\frac{d^2\mathscr{E}_1}{d\omega\, do} = 0.38e^2K^2\gamma^2c^{-1}$$

at $p_\perp = 1.2$ (the regime of optimal fields in the undulator[17,57,87]), after which it begins to drop gradually.

At $p_\perp = 1.45$ the energies of the first and third harmonics are equal. On further increase of $p_\perp$ the maximum of the radiation shifts to higher harmonics. At the same time, in accordance with Eq. (4.18), there is a rise of the frequency at which the maximum energy of the radiation occurs.

The widths of the angular distributions of undulator radiation for $p_\perp \lesssim 1$ are commensurate in the two transverse directions and are of the order γ^{-1}.[17,57] In the plane of the oscillations of the particles, with increase of the angle ϑ, the radiation of each harmonic passes through a series of maxima and minima whose number increases with increase of the number of the harmonic.

The number of maxima observed on variation of the azimuthal angle φ is always even; for the higher harmonics it is higher than for the fundamental harmonic and increases with increase of the harmonic number. We note that the electric field vector **e** of the radiation in the x,z plane for all harmonics lies in this plane. For the vertical plane this vector is parallel to the x,z plane for odd harmonics and normal to it for even harmonics.

For $p_\perp = 1$ for small angles ($\vartheta \ll 1$) the principal energy of the radiation is in the first harmonic. However, already at $\vartheta \gtrsim 1/2$ the energy of the radiation in the second and higher harmonics is comparable and even exceeds the radiation energy in the first harmonic. The angular distribution in the vertical plane ($\varphi = \pi/2$) is characterized by a simpler law of variation—one maximum for the odd harmonics and two maxima for the even harmonics. An increase of the field in the undulator is accompanied by broadening of the angular distribution of the radiation in the plane of oscillations, which is due mainly to the increase of the radiation in the higher harmonics.

Let us consider now the change of the spectral distribution with increase of the field in the undulator, assuming that $K \gg 1$.[17,57,87] For an optimum value of the field in the undulator ($p_\perp \approx 1$; Fig. 7a) the width of the "line" of the first harmonic at half-height is about 25% of the total width, the energy of the radiation in the second harmonic reaches ~30%, and in the third harmonic about 15% of the radiation energy at the maximum of the first harmonic.

On a further increase of the magnetic field the fraction of the radiation associated with higher harmonics rises. In Fig. 7b we have shown the spectral distribution of radiation for $p_\perp = 2.0$. In contrast to the distribution at zero angle, here the maximum in the spectrum occurs in the first harmonic.

In the limiting case of strong fields ($p_\perp \gg 1$) in the undulator[21,86–89] (or of high energies in the radiation of channeled particles in a crystal) the radiation at the point of observation in the xz plane comes only from those portions of the trajectory on extension of which the particle velocity vector rotates by an angle of the order γ^{-1} with respect to the direction of observation; see Eq. (4.1). On a screen placed at a

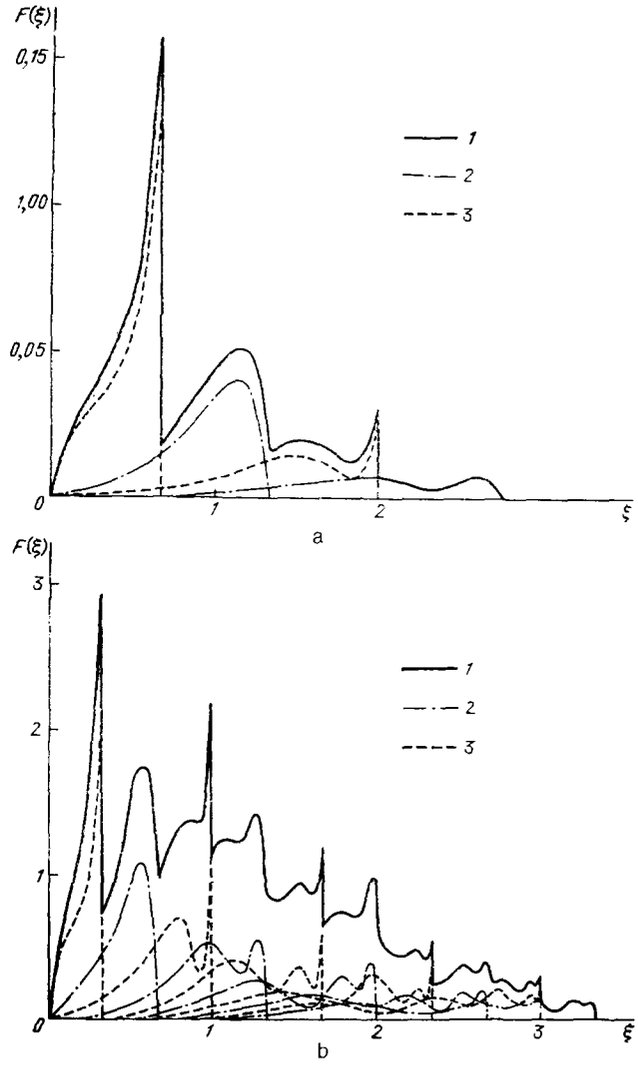

FIG. 7. Spectral distribution of radiation in a planar undulator for $p_\perp = 1.0$ (a) and $p_\perp = 2.0$ (b). Curve 1–combined radiation, curve 2–radiation in even harmonics, curve 3–radiation in odd harmonics.

distance R from the undulator, the radiation spot of size $R\gamma^{-1}$ shifts horizontally, illuminating a narrow band of length $R\alpha_m$.

Carrying out in (4.18) the limiting transition, we find for the radiation energy along the undulator axis ($\omega = \omega_{(2p+1)m}$, $\vartheta = 0$) (Ref. 88):

$$\frac{d^2\mathscr{E}}{d\omega\, do} = \frac{3K^2e^2\gamma^2}{c}\left[\frac{2}{\pi}(2p+1)\,\eta_0 K_{2/3}((2p+1)\,\eta_0)\right]^2, \quad (4.19)$$

where

$$\eta_0 = 2\left[3p_\perp\left(1+\frac{p_\perp^2}{2}\right)\right]^{-1},$$

and $K_{2/3}$ is the Macdonald function. For $(2p+1)\eta_0 = 0.5$, this energy takes on a maximum value equal to $0.45K^2e^2\gamma^2c^{-1}$ which does not depend on the undulator field strength. The maximum in the spectrum occurs at harmonic k_m and frequency ω_m,

$$k_m = \frac{3}{8}p_\perp^3, \quad \omega_m = \frac{3}{2}p_\perp\Omega\gamma^2 = \frac{3eH_m\gamma^2}{2mc}. \quad (4.20)$$

The number k_m does not depend on the electron energy, and the corresponding frequency ω_m coincides with the critical frequency of radiation in a uniform magnetic field H_m. We note that the maximum value of the spectral and angular energy distribution of radiation along the undulator axis for strong fields is 15% higher than at the optimum field, since with increase of the field the main increase is in the fraction of energy radiated at large angles with respect to the undulator axis. The integrated radiation spectrum in a strong field is close in shape to the synchrotron-radiation spectrum.

Frequencies $\omega \sim \Omega\gamma^2$ characteristic of the optimal fields in the undulator correspond in the case of strong fields to harmonics with numbers $k_{opt} \approx p_\perp^2$ such that $k_{opt}\eta_0 \ll 1$. Using the approximate expression for the Macdonald function, we obtain for the radiation at frequency $\omega_{2p+1} \approx \Omega\gamma^2$, and $\vartheta = 0$ (Ref. 88)

$$\frac{d^2\mathscr{E}}{d\omega\, do} = \frac{2\cdot 6^{1/3}\Gamma^2(2/3)}{\pi^2}\,\frac{K^2e^2\gamma^2}{c}\,p_\perp^{-2/3}. \quad (4.21)$$

Thus, with increase of the field while the undulator period remains constant the radiated energy in the line in the frequency region discussed falls off as $H_m^{-2/3}$. Therefore undulators with high fields can be advantageously used for operation at frequencies significantly greater than $\Omega\gamma^2$.

4.4. Radiation in a helical undulator. In a helical undulator in accordance with the form of the particle trajectory (3.9) the angular distribution of the radiation is axially symmetric. As in a planar undulator, in the direction of its axis there is no radiation of even harmonics, and of the odd harmonics only the first is present, which is completely circularly polarized. The spectral and angular distribution of the radiation in the dipole approximation differs from the expression (4.17) only in the fact that in it we have in place of $\cos^2\varphi$ a factor 1/2. In regard to the spectral distribution, it has the same form as in the case of a planar undulator. In the general case the spectral and angular energy distribution of the radiation can be written in the form[17,18,21,90-93]

$$\frac{d^2\mathscr{E}}{d\xi\, do} = \frac{6\mathscr{E}\gamma^2}{\pi^3 K}\sum_{k=1}^{\infty}\frac{\sin^2\pi Kk\,[(\xi/\xi_k)-1]}{k^2\,[(\xi/\xi_k)-1]^2}\,\xi^2 F_k(\theta),$$

$$F_k(\theta) = J_k'^2(k\varkappa) + \left(\frac{T}{\varkappa}\right)^2 J_k^2(k\varkappa), \quad (4.22)$$

$$\varkappa(\vartheta) = \frac{\sqrt{2}\,\vartheta p_\perp}{1+\vartheta^2+(p_\perp^2/2)}, \quad T = \frac{1-\vartheta^2+p_\perp^2/2}{1+\vartheta^2+(p_\perp^2/2)},$$

where

$$\mathscr{E} = \frac{e^2\Omega^2 p_\perp^2\gamma^2}{3c}\,\frac{K\lambda_0}{\beta_\parallel c}$$

is the total energy of the radiation and J_k and J_k' are the Bessel function and its derivative; as before

$$\xi = \frac{\omega}{2\Omega\gamma^2}, \quad \vartheta = \theta\gamma.$$

The radiation spectrum from the k-th harmonic in motion of an electron along a right-handed helical line we shall represent in the form of the sum of radiation with right-handed (+) and left-handed (−) circular polarization ($K \gg 1$)[18,91,93]:

$$\frac{d\mathscr{E}}{d\xi} = 6\mathscr{E}\xi\,(W_{k+}(\xi) + W_{k-}(\xi)), \quad (4.23)$$

$$W_{k\pm} = \frac{1}{2}\left(J_k'(k\varkappa) \pm \frac{2\eta\xi - k}{k\varkappa}J_k(k\varkappa)\right)^2;$$

here

$$\varkappa(\xi) = \frac{\sqrt{2}}{k}p_\perp[\xi(k-\eta\xi)]^{1/2}, \quad \eta = 1+\frac{p_\perp^2}{2}.$$

The conditions of generation become optimal when the spectral and angular distribution or the angular distribution of the energy of radiation of the first harmonic reaches a maximum. According to (4.22) and (4.23) the spectral and angular distribution of the radiation energy has a maximum at $p_\perp = \sqrt{2}$, and the angular distribution has a maximum at $p_\perp = 1$.[57,91,93] For $p_\perp = 1$, as in a planar undulator, there is a sharply expressed peak in the spectrum, which corresponds to the radiation of the fundamental. On the other hand the spectral distributions of the higher harmonics are distinguished by a greater smoothness. The degree of circular polarization at the maximum of the spectrum reaches about 80%. Within the peak it passes through zero and for low-frequency photons has the opposite sign. For the optimal field a large part of the radiated energy is concentrated near the undulator axis in the range of angles $\Delta\vartheta = 1/2$, where mainly the first harmonic is radiated. For the radiation included inside a cone with $\vartheta \leqslant 1/2$, a high degree of circular polarization $p \sim 95\%$ is characteristic. In the remaining directions the radiation is elliptically polarized with a ratio of the semiaxes of the polarization ellipse[17,18]

$$\frac{b}{a} = \frac{\varkappa J_k'(k\varkappa)}{J_k(k\varkappa)}. \quad (4.24)$$

It follows from this formula that near the surface of a cone with opening angle

$$\theta = \frac{1}{\gamma}\left(1+\frac{p_\perp^2}{2}\right)^{1/2}$$

the radiation in a helical undulator becomes linearly polarized. The plane of its polarization is tangent to the surface of the cone. This is rather obvious, since in the co-moving system with observation at corresponding angles a circle appears to be a straight line.

In contrast to the planar case, with increase of the field in a helical undulator the radiation departs from its axis. At higher fields the ray of undulator radiation describes a conical surface with an angle at the vertex of the cone α_m. On a

TABLE I.

E, GeV	0,1	1	10	50	100	400	10^3	$5\cdot10^3$
$\hbar\omega$, keV	$1{,}58\cdot10^{-3}$	0,158	15,8	395,6	$1{,}58\cdot10^3$	$25{,}32\cdot10^3$	$158\cdot10^3$	$3{,}96\cdot10^6$

screen the undulator spot will move uniformly around a circle of radius $R\alpha_m$, where R is the distance from the undulator to the screen.

4.5. Basic energy relations. Here we shall dwell only on relations which permit quantitative evaluation of the characteristic values of the principal parameters of undulator radiation sources constructed on the basis of a planar undulator. Similar relations for a helical undulator can be obtained by simple replacement of H_m by $\sqrt{2}H_m$ (see also Refs. 94 and 95).

The maximum energy of photons of the k-th harmonic is

$$\hbar\omega_k(\mathrm{KeV}) = \frac{0{,}949k\,(E(\mathrm{GeV})^2}{[1+(p_\perp^2/2)]\,\lambda_0(\mathrm{cm})}, \tag{4.25}$$

where $p_\perp = 0.0934H_m$ (kOe) λ_0 (cm).

The energy of the photons at the maximum of the spectrum of the principal harmonic for an undulator with a characteristic period $\lambda_0 = 4$ cm and an optimal field $H_m = 2.65$ kOe ($p_\perp = 1$) are given in the following table.

Undulator radiation has its own characteristic scale invariance. For example, the total energy of radiation in a given region of the spectrum will depend only on the reduced frequency $\xi = \omega/2\Omega\gamma^2$. A consequence of this fact is that the form of the spectral distribution (in ξ) of the number of emitted photons is independent of the energy of the electrons. For the number of photons with energy

$$\hbar\omega_{(2p+1)m} = \frac{2\,(2p+1)\,\hbar\Omega\gamma^2}{1+(p_\perp^2/2)},$$

emitted at zero angle on traversal of the undulator by a single electron, we have [see Eq. (4.10)]

$$\frac{d^2N_{2p+1}}{d\omega\,do} = \frac{\alpha K^2\lambda_0}{4\pi c}\,\frac{1+(p_\perp^2/2)}{2p+1}\,F_{2p+1}(p_\perp), \tag{4.26}$$

where $\alpha = e^2/\hbar c$ is the fine-structure constant.

The radiation per unit time of an electron beam with a current of 1 A in a frequency interval of width 1% from $\omega_{(2p+1)m}$ into an angle of 1 (mrad)^2 is

$$\frac{dN_{2p+1}/dt}{d\omega/\omega\,do_{\mathcal{S}}} = 3{,}52\cdot10^{15}\,(E(\mathrm{GeV}))^2 I\,(A)\,K^2F_{2p+1}(p_\perp)$$

$$\left(\frac{\text{photons}}{\text{sec}\cdot\text{mrad}^2\cdot1\%}\right); \tag{4.27}$$

its form for the first few harmonics is shown in Fig. 7. The total radiation power summed over all harmonics in an undulator is

$$W(\text{watts}) = 0.127(E(\mathrm{GeV}))^2\langle(H(\mathrm{kOe}))^2\rangle L(\mathrm{cm})I(\mathrm{A}), \tag{4.28}$$

where $\langle H^2\rangle$ is the average of the square of the field in the period of the undulator. For a planar undulator $\langle H^2\rangle = (1/2)H_m^2$, and for a helical undulator $\langle H^2\rangle = H_m^2$.

4.6. Quantum corrections to undulator radiation. The region of applicability of classical electrodynamics is limited by the condition of smallness of the energy of the radiated photon in comparison with the electron energy $\hbar\omega/\mathscr{E} \ll 1$, where $\hbar$ is Planck's constant.

For moderately relativistic transverse motion ($p_\perp \lesssim 1$) the energy of a photon radiated in an undulator is $\hbar\omega \sim \hbar\Omega\gamma^2$ and the quantum effects of the radiation are conveniently characterized by the parameter[17,78]

$$\chi = \frac{2\hbar\Omega\gamma^2}{\mathscr{E}} = 2\frac{\lambda_{ce}}{\lambda_0}\gamma, \tag{4.29}$$

where $\lambda_{ce} = h/mc = 2.426\cdot10^{-10}$ cm is the electron Compton wavelength.

For ultrarelativistic transverse motion ($p_\perp \gg 1$) the quantum effects in the undulator appear in the same way as in motion in a uniform magnetic field. Here the condition of applicability of the classical theory is

$$H_m\gamma \ll H_c, \tag{4.30}$$

where $H_c = m^2c^3/e\hbar = 4.4\cdot10^{13}$ Oe.

The influence of quantum effects at low fields is traced especially easily for the case of an undulator with a plain electro-magnetic wave. In such an undulator the wave with frequency ω_b and a relativistic electron move opposite to each other. The energy of the photon emitted at an angle θ with respect to the direction of motion of the electron is

$$\omega = \frac{2\omega_b}{1-\beta\cos\theta+(\omega_b/\mathscr{E})\,(1-\cos\theta)}; \tag{4.31}$$

here and below in this section we shall set $\hbar = c = 1$. The maximum energy ω_m is observed for photons scattered in the direction of motion of the electron (Compton backscattering):

$$\omega_m = \frac{\mathscr{E}\chi}{1+\chi}, \tag{4.32}$$

where it has been taken into account that for a relativistic particle in the field of a wave $\Omega = 2\omega_b$ For $\chi \ll 1$ this expression goes over into the classical formula

$$\omega_m = 4\omega_b\gamma^2. \tag{4.33}$$

As the electromagnetic wave we can use photons previously emitted by a beam in an undulator and then reflected from a mirror. A source of photons can be also colliding electron or positron beams. This leads to emission of energetic photons: $\omega_b \approx 2\Omega\gamma^2$, $\omega_m \approx 8\Omega\gamma^4$.

The quantum nature of the transverse motion of the electrons appears when they are propagated in the quadrupole fields of electromagnetic lenses or crystals if the phase space of the transverse motion is insufficiently large, $p_\perp x_m \lesssim \hbar$.[80]

5. RADIATION FROM A BEAM OF PARTICLES IN AN UNDULATOR

5.1. Influence of electron-beam parameters and diaphragming of undulator radiation on its properties. Previous-

ly we have discussed the properties of the radiation of a single particle moving along the undulator axis. We shall now discuss the properties of UR emitted by a beam of particles.

We shall place in correspondence with each particle a point in six-dimensional phase space, the location of which is given by the transverse coordinates x,y, the angles (x',y') formed with the undulator axis, the longitudinal coordinate z with respect to the center of the beam, and the deviation of its energy from the average. As a rule, this distribution can be described by a Gaussian law with the following dispersions: $\sigma_x^2, \sigma_y^2, \sigma_{x'}^2, \sigma_{y'}^2, \sigma_z^2, \sigma_\gamma^2$. The emittance in a given plane of motion is defined as the product of the standard deviations of the displacements and angles of the particles with respect to the beam axis ($\varepsilon_{x,y} = \pi\sigma_{x,y}\sigma_{x',y'}$). Here it is assumed that the center of the beam is always on the undulator axis.

The experimentally observed characteristics of undulator radiation (differential or integral) are determined not only by the beam parameters but also by the acceptance of the experimental apparatus: by the shape of the entrance aperture and its dimensions r_x and r_y. The angular interval of the radiation in the direction of observation selected by the entrance aperture of the experimental apparatus is

$$\Delta\theta_{\text{д}d,\,y} = \frac{r_{x,\,y}}{l}, \quad \Delta\theta_d = (\Delta\theta_{dx}^2 + \Delta\theta_{d,y}^2)^{1/2}, \quad \Delta\vartheta_d = \gamma\Delta\theta_d. \tag{5.1}$$

In a number of cases the beam parameters are more conveniently described by the width of the effective angular distribution at halfheight[96]:

$$\Delta\theta_e = 2\sqrt{2\ln 2}\,\sigma_e \approx 2{,}36\,\sigma_e, \tag{5.2}$$

$$\sigma_{ex'} = \left[\sigma_{x'}^2 + \left(\frac{\sigma_x}{l}\right)^2\right]^{1/2},$$

$$\sigma_{ey'} = \left[\sigma_{y'}^2 + \left(\frac{\sigma_y}{l}\right)^2\right]^{1/2}, \quad \sigma_e^2 = \sigma_{ex'}^2 + \sigma_{ey'}^2, \tag{5.3}$$

where l is the distance from the center of the undulator to the point of observation.

a) The influence of the beam parameters on the spectral and angular characteristics of the undulator radiation becomes appreciable if $\Delta\vartheta_e$ ($\Delta\vartheta_e = \phi\Delta\theta_e$) approaches in order of magnitude $\Delta\vartheta_k$ ($\Delta\vartheta_k = \gamma\Delta\theta_k$ (4.9)). In observation of radiation along the undulator axis this condition takes the form $\Delta\vartheta_e \lesssim \Delta\vartheta_{k0}$ [see Eq. (4.10)]. As follows from (4.9) and (4.8), the sensitivity of the properties of the radiation to the beam parameters becomes greatest for $\lambda = \lambda_{km}$ $[2 + (p_\perp^2/2)]$, when $\vartheta_m = \gamma\theta_m = 1$.

We note that the width $\Delta\vartheta$ at half-height of the angular distribution of the radiation in the selected plane (x,z or y,z) will depend mainly on the angular spread of the particles in this same plane, and for $\Delta\vartheta_{ex'y'} > \Delta\vartheta_k$ it will be proportional to $\sigma_{ex',y'}$.[28,96]

Broadening of the angular distribution of undulator radiation will occur also with increase of the energy spread $\Delta\gamma$. For $\vartheta_m \sim 1$ it is proportional to $\Delta\gamma/\gamma$ ($\Delta\vartheta \sim \{[2 + (p_\perp^2/2]/2kK\}\Delta\gamma/\gamma$).

For $\vartheta_m \gtrsim \Delta\vartheta_{k0}$ an increase of the spread $\Delta\vartheta_e$ of the particles in the beam will lead also to a shift of the maximum of the spectral and angular intensity of the radiation toward smaller angles. This shift $\Delta\vartheta_m$ in the selected plane will depend on the angular spread of the particles in the plane perpendicular to it and for $\vartheta_m \gg \sigma_{ex',y'}$ its magnitude is proportional to $\sigma_{ex',y'}^2/\vartheta_m$. In the general case $\Delta\vartheta_m$ will depend also on the angular distribution of the vector $\mathbf{a}_k(\vartheta,\varphi)$ in (4.4).

b) The width of the spectral line of undulator radiation, with inclusion of the energy and angular spread of the particles in the beam and also of the angular acceptance of the diaphragm, can be estimated from the expression

$$\frac{\Delta\lambda}{\lambda} \approx \left\{\left(\frac{1}{kK}\right)^2 + \left[\frac{\Delta\vartheta_e^2 + \Delta\vartheta_{\text{д}}^2}{1 + (p_\perp^2/2)}\right]^2 + \left(\frac{2\Delta\gamma}{\gamma}\right)^2\right\}^{1/2}. \tag{5.4}$$

The intensity of radiation propagated at zero angle at wavelength λ_{km}, with opening of the angle selected by the diaphragm $\Delta\vartheta_d$ up to

$$\Delta\vartheta_{k0} = \left[\frac{1 + (p_\perp^2/2)}{kK}\right]^{1/2}$$

increases without substantial broadening of the line. Optimal conditions for monochromatization of undulator radiation by means of a diaphragm can be written in the form[96]

$$\Delta\vartheta_e \sim \Delta\vartheta_d \lesssim \Delta\vartheta_{k0} \quad (p_\perp \lesssim 1). \tag{5.5}$$

We note that in the optical region of the spectrum the separation of monochromatic radiation can be accomplished also by means of a mirror. The requirements on the angular size of the mirror are given by the same conditions (5.5). It follows from this that in a number of experiments which do not require very high monochromatization of the beam of radiation it is possible to use undulator radiation without a monochromator.[15,64]

It is important to mention that the energy spread of the particles leads to a symmetric broadening, while the angular spread leads to deformation of the spectral distribution curve of the radiation. The distibution becomes asymmetric with a flatter falloff on the long-wavelength side.[96,97]

For finite sizes of the beam cross section a broadening of the spectral line of undulator radiation can be produced also by inhomogeneity of the undulator magnetic field in the gap between poles. This inhomogeneity can be described by the following formula:

$$p_\perp = p_{\perp 0} + p_{\perp 1}y + \frac{1}{2}p_{\perp 2}y^2 + \ldots,$$

where

$$p_{\perp 1} = \frac{\partial p_\perp}{\partial y}, \quad p_{\perp 2} = \frac{\partial^2 p_\perp}{\partial y^2}.$$

For symmetric magnetic fields ($p_\perp(-y) = p_\perp(y)$) in the expression for $p_\perp$ the linear term disappears ($p_{\perp 1} = 0$), and in the case, for example, of a planar undulator[29,96,98] the broadening of the line amounts to

$$\frac{\Delta\lambda}{\lambda} = \frac{p_{\perp 0}^2/2}{1 + (p_{\perp 0}^2/2)}\left(\frac{1}{H_m}\frac{\partial^2 H_m}{\partial y^2}\right)\sigma_y^2, \tag{5.6}$$

where $(1/H_m)\partial^2 H_m/\partial y^2$ is of order $1/\lambda_0^2$.

Existence of an angular spread of the electrons leads also to appearance in the direction of the axis of a planar undulator of radiation in even harmonics.

c) One of the important characteristics of a source of electromagnetic radiation is its brightness in a given portion of the spectrum, i.e., the intensity per unit area of the radiating surface of the source per unit solid angle. The area S of the radiating surface of a beam of particles in an undulator will depend on its transverse dimensions, the angular spread, the length of the undulator, and the angle of observation:

$$S = \pi \Delta_x \Delta_y \quad (\theta \ll 1), \tag{5.7}$$

where

$$\Delta_{x,y} = \left[\sigma_{x,y}^2 + \left(\frac{1}{4}\sigma_{x',y'}^2 + \theta^2\right) L^2 + d_k^2\right]^{1/2}$$

are the visible horizontal and vertical dimensions of the beam. In the direction $\theta = 0$ it takes on a minimum value for $\sigma_{x',y'} = (2\varepsilon_{x,y}/\pi L)^{1/2}$.

The spectral energy of radiation per unit solid angle in the direction $\theta = 0$ decreases with increase of the angular spread of the beam in inverse proportion to the square of the broadening of the angular distribution of the radiation:

$$\frac{\Delta\theta_{x,y}}{\Delta\theta_{k0}} = \left(1 + \frac{\sigma_{x',y'}^2}{\Delta\theta_{k0}^2}\right)^{1/2}.$$

Then, according to Eq. (5.7), the spectral brightness of a source of undulator radiation in this direction is determined by the expression [18,85]

$$B(\lambda, \theta = 0) = \frac{d^2 I_n / d\lambda\, do}{\pi \Delta_x \Delta_y [1 + (\sigma_{x'}^2/\Delta\theta_{k0}^2)]^{1/2} [1 + (\sigma_{y'}^2/\Delta\theta_{k0}^2)]^{1/2}} \quad (\lambda, \theta = 0), \tag{5.8}$$

where

$$\frac{d^2 I_n}{d\lambda\, do} = \frac{J}{e} \frac{d^2 \mathscr{E}}{d\lambda_0\, do} -$$

is the spectral and angular intensity of the radiation along the undulator axis of a beam with current J and with zero emittance.

d) In a planar undulator the angular spread leads to a decrease of the linear polarization of the radiation. For radiation propagating near the undulator axis ($\lambda \sim \lambda_{km} [1 + (p_1^2/2)]$, the ratio of the polarization components will depend on both the horizontal and vertical angular spreads[96]:

$$\frac{g_\perp}{g_\parallel} \sim 4\gamma^4 \sigma_{ex'}^2 \sigma_{ey'}^2. \tag{5.9}$$

With deviation from the undulator axis by an angle $\vartheta_m \sim 1$ ($\lambda \sim \lambda_{km} [2 + (p_1^2/2)]$), the polarization of the radiation at an azimuth $\varphi = \pi/2$ is determined mainly by the angular spread in the plane of oscillations of the particles ($\varphi = 0$)

$$\frac{g_\perp}{g_\parallel} \sim \gamma^2 \sigma_{ex}^2, \quad \sigma_{ex} \ll \frac{1}{\gamma}. \tag{5.10}$$

When the optimal conditions (5.5) for monochromatization exist, the radiation preserves a high degree of linear polarization, of the order of 0.99 or higher.

In motion of a particle in a helical undulator the angular spread of the particles in the beam leads to a decrease of the degree of circular polarization. For example, along the undulator axis ($\theta = 0$)[96]

$$\frac{g_-}{g_+} \sim \gamma^4 (3\sigma_{ex'}^4 + 2\sigma_{ex'}^2 \sigma_{ey'}^2 + 3\sigma_{ey'}^4), \tag{5.11}$$

where g_+ and g_- are the components corresponding to right-handed and left-handed polarization.

A more detailed analysis of the radiation properties of real beams in an undulator can be found in Refs. 96 and 99.

5.2. Conditions of generation of coherent undulator radiation. A beam of charged particles moving in an undulator is a set of oscillators whose oscillation phases in the general case depend on the relative location of the particles in the beam and on the angle of their entry into the undulator. Under certain conditions the phases of the electromagnetic waves emitted by individual particles in an undulator can be matched and grouped about some specific phase, i.e., the particles of the beam will radiate coherently in a given direction.

We shall consider the basic properties of generators of coherent undulator radiation, among which are sources of spontaneous coherent and induced undulator radiation.

5.2.1. Spontaneous coherent undulator radiation. To obtain spontaneous coherent radiation a beam must be grouped in bunches with small longitudinal and transverse dimensions[100]

$$z_e \ll \lambda_{km}, \quad x_e \approx y_e \ll \lambda_{km}\gamma \tag{5.12}$$

and must have small angular and energy spreads

$$\Delta\theta_e < \Delta\theta_{k0}, \quad \frac{\Delta\gamma}{\gamma} < \frac{1}{kK}. \tag{5.13}$$

The intensity of the radiation of such a beam is proportional to the square of the number of particles in it. A beam of charged particles consisting of a series of bunches and which satisfies these conditions will emit coherent undulator radiation which in addition to high intensity will have a higher directivity and monochromaticity in comparison with the radiation of a single bunch.

The technique used at the present time for formation of short electron bunches with length ~ 0.1 mm (Ref. 101) provides the possibility of producing generators of submillimeter waves with output power about 10^5 W. By using the effect of grouping of a particle beam during its passage through matter,[102] it is possible to achieve the generation of coherent undulator radiation also in the region of shorter wavelengths.

For not too great deviations from the conditions (5.12) and (5.13) the total energy of the radiation will remain substantially above the energy of incoherent radiation. In this case one speaks of partially coherent undulator radiation, the properties of which have been considered in detail in Refs. 100 and 103.

We mention that in coherent radiation the energy loss of the particles may become so large that it becomes necessary to take into account the influence of the loss both on the dynamics of the particles and on the properties of the radiation itself.

5.2.2. Spatial coherence of undulator radiation. The radiation of a beam of charged particles in an undulator, like the radiation of other quasimonochromatic light sources, has the property of spatial coherence. The degree of spatial coherence of undulator radiation, which characterizes the relation of the phases of the electromagnetic oscillations at various points of observation, depends on the size and shape of the charged-particle beam and also on the angular and energy spreads of the particles in the beam.[104] It takes on its maximum value when the conditions (5.12) and (5.13) are satisfied. One must keep in mind that for any given direction the region of spatial coherence of the radiation is restricted to an interval of angles $\Delta\theta_k$ given by (4.9).

For small angular and energy spreads (5.13) the degree of spatial coherence of undulator radiation will depend only

on the transverse size of the particle beam. For a uniform distribution of the particles in a beam cross section having the shape of a circle of radius r_e, the electromagnetic waves emitted along the undulator axis will be coherent in the interval of angles[104]

$$\Delta\theta_{coh} < \frac{\lambda}{r_e}. \tag{5.14}$$

It is important to mention that sources of undulator radiation permit one to obtain a high degree of spatial coherence of the radiation without preliminary monochromatization of the radiation and may find application in the holography of microscopic objects.

5.3. Induced processes in an undulator. Let us consider the interaction of an electron beam with a plane electromagnetic wave of wavelength λ propagating along the undulator axis, neglecting effects due to space charge of the beam,—the "Compton regime." Interaction of the beam of electrons with the wave can lead to exchange of energy between them. The transverse component of the particle velocity interacts with the electric field of the wave. The intensity of the interaction depends on their relative orientation, i.e., on the ratio of the phases of oscillations of the particle and the wave.

For definiteness we shall consider the motion of a particle in a helical undulator and we shall assume the electromagnetic wave to be circularly polarized with an electric field vector rotating in the same direction as the beam particles. In Sec. 2.4 we derived the condition of synchronism of the wave and the particle. If the frequency of the wave is given, this condition determines the energy

$$\gamma_s = \left\{ \frac{\lambda_0 [1 + (p_\perp^2/2)]}{\lambda} \right\}^{1/2} \tag{5.15}$$

of a synchronous particle. Particles with a different energy $\gamma = \gamma_s + \Delta\gamma$ in the absence of a wave will be displaced with respect to a synchronous particle with a velocity

$$c\Delta\beta = c\left(1 + \frac{p_\perp^2}{2}\right)\gamma_s^{-3}\Delta\gamma. \tag{5.16}$$

Here particles with higher energy will lead the synchronous particle, and those with lower energy will lag it. The presence of an external wave leads to a change of this picture. In Fig. 8 we have shown a projection of the particle trajectories on the plane perpendicular to the axis of a helical undulator, and also the orientation of the electric-field vector of the wave at some moment of time.[42,56] For particles with the synchronous energy with the passage of time this picture will rotate as a whole around the undulator axis. In the trajectory there are distinguished particles: 2 and 4, the transverse velocity of which is directed normal to the electric field vector of the wave $\mathbf{E}_b$. The energy of such particles is conserved. The velocity vector of particle 3 is directed along the electric

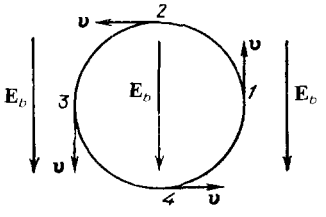

FIG. 8. Motion of particles with various phases in the fields of a plane circularly polarized wave and of a helical undulator.

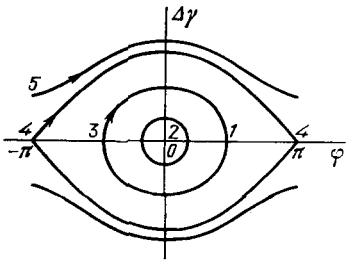

FIG. 9. Phase motions of particles in free electron lasers.

field vector, and that of particle 1 is opposite to it. Therefore in accordance with the formula[52] $d\mathscr{E}/dt = e(\mathbf{E}_b\mathbf{v})$ particle 3 will be accelerated and its energy will increase, while particle 1 will slow down and lose energy to electromagnetic radiation. Therefore as the result of interaction with the wave in a homogeneous initially monoenergetic beam uniformly distributed along the undulator axis there will appear an energy spread which in turn leads to a relative displacement of the particles in the longitudinal direction.

The relative motion of the particles and the change of their energy can be conveniently represented in phase plane $\Delta\gamma, \varphi$ (Fig. 9).[42,45,81,105] As abscissa we plot the phase of the particles $\varphi = 2\pi\Delta z/\beta_\parallel\lambda$ (Δz is the displacement with respect to a synchronous particle), and the phase of the equilibrium particle 2 is taken as zero. As ordinate we plot the deviation $\Delta\gamma$ of the energy from the equilibrium value γ_s. Particles 1 and 3 will execute phase oscillations about the equilibrium phase of particle 2: We have here the mechanism of phase stability, which is well known in accelerator theory, and a certain fraction of the particles are captured by the wave. However, not nearly all particles will be captured by the wave. For example, particle 5, which initially had the same phase as particle 4 but a somewhat larger (or smaller) energy γ_5 will be accelerated (or slowed down) by the wave and will be displaced in phase. Going over to the region of retarding phases, this particle will slow down to the initial energy γ_5. Subsequently the nature of the motion is preserved and the phase of such particles will increase up to the moment of departure from the undulator. The curves drawn through the point 4 divide the phase plane into two regions: In the inner region we have particle motion bounded in phase, and in the external region it is unbounded. The curve which separates these two regions is called the separatrix. The size of the separatrix obviously will depend on the amplitude of the external wave. A monoenergetic beam of particles with the equilibrium energy on the average does not exchange energy with the wave: as many particles are slowed down as are accelerated

Transfer of energy to the wave can be accomplished if we select a beam-particle energy above the equilibrium energy by some amount $\Delta\gamma$. Through a half-period of the phase oscillations the energy of the beam particles will decrease by about $2\Delta\gamma$ and will become below the equilibrium value. The energy lost by the beam will be expended on amplification of the external wave.

In order to accomplish the generation of induced radiation, one places the mirrors of an optical resonator on the undulator axis. In the resonator there is storage and amplification of spontaneous undulator radiation. Its high directivity with comparatively small size of the resonator mirrors

permits retention of the main part of the energy of spontaneous radiation of a given wavelength. In selection of the geometry of the optical resonator the diffraction size of the radiator in the undulator (4.11) is taken into account. It is obvious that here, in contrast to free space, a discrete set of electromagnetic waves (modes) will be excited. The distance between the mirrors is chosen so as to synchronize the electron bunches with the optical pulses of radiation from the neighboring bunches of the beam. The monochromaticity of the radiation is determined by the extent of the electron bunches.

Devices working on this principle are usually called free electron lasers (FEL), in contrast to ordinary lasers in which bound atomic electrons are used. The active medium in a free electron laser is the electron beam, and the spatially periodic field of the undulator is the pumping field.[106] The advantage of such a generator consists of the possibility of smooth tuning of the wavelength of the generated radiation by changing the amplitude of the undulator magnetic field or the electron energy.

The gain of the free electron laser is defined as the ratio of the increment ΔI of the intensity of the radiation field in the undulator length to the intensity I at the input to the undulator: $G = \Delta I / I$. As has been shown in Refs. 105, 107, and 108, in the weak signal regime ($\Delta I \ll I$) the gain for an unmodulated electron beam is proportional to the steepness of the spectral line of spontaneous undulator radiation for the identical state of polarization of the amplified and spontaneous radiation. This property indicates the direct connection of the parameters of a free electron laser with the spectral and angular characteristics of the spontaneous radiation, which is characteristic of induced radiation.[109]

For radiation propagated at an angle θ to the direction of motion of a monoenergetic beam, the gain at a fixed wavelength λ can be written in the form

$$G_k = \frac{J}{J_A} \frac{4\pi^2 K^3 \lambda_0 \lambda}{S\gamma} \frac{p_\perp^2}{2} \left(1 + \frac{p_\perp^2}{2}\right)$$

$$f_k(\lambda, \vartheta, \varphi) \frac{\partial}{\partial \sigma_k} \left(\frac{\sin \sigma_k}{\sigma_k}\right)^2 \qquad (5.17)$$

where

$$\sigma_k = \pi k K \left(\frac{\lambda_k}{\lambda} - 1\right), \quad \lambda_k = \frac{\lambda_0 [1 + \vartheta^2 + (p_\perp^2/2)]}{2k\gamma^2},$$

J is the beam current, $J_A = mc^3/e$ is the Alfvén current, S is the beam cross section, which does not exceed the cross section of the wave, and the function $f_k(\lambda, \vartheta, \varphi)$ describes the angular distribution of the intensity of spontaneous undulator radiation at wavelength λ. The last factor in (5.17) determines the well known dependence of the gain on the energy of the electron beam and the wavelength of the radiation.

According to (5.17) the gain is an odd function of σ_k which vanishes at $\sigma_k = 0$ ($\lambda = \lambda_k$) and takes on positive values for $\sigma_k < 0$ (the long-wavelength part of the spectral line of undulator radiation $\lambda > \lambda_k$). The gain reaches its maximum value at a wavelength

$$\lambda = \frac{\lambda k_m}{1 - (1{,}3/\pi k K)}. \qquad (5.18)$$

With decrease of the wavelength it drops as $\lambda^{3/2}$, which limits the possibility of creating short-wavelength generators.

The gain of a free electron laser depends both on the undulator parameters and on the particle-beam parameters. In particular, the existence of an angular spread of the particles in the beam leads to a slower falloff of the intensity of radiation in the long-wavelength region of the spectrum and consequently to a shift of the maximum of the gain toward the long-wavelength region and to an appreciable decrease of this maximum.[110] Therefore to preserve a high level of gain it is necessary that this shift lie within the spectral line of the spontaneous radiation.

The interaction of the electron beam with the wave in a free electron laser is accompanied by its modulation in energy in the longitudinal direction, which when there is a sufficiently long drift space beyond the undulator goes over to a longitudinal modulation of the beam density with the period of the wave λ. In free space the maximum modulation of the density occurs in traversal of a drift region of length $L_D \approx \lambda \gamma_s^3 / 4\Delta\gamma$. Passage of a beam of electrons modulated in this way through a subsequent undulator permits substantial increase of the gain of the external wave.[111,112] Sometimes it may turn out to be useful to use as the grouping element an undulator with parameters which change smoothly along its length[115] or to make use of grouping in a long undulator under the action of the undulator's own radiation.[75,114,115]

A significant increase of the gain can be achieved in an optical klystron (OK), proposed at the Institute of Nuclear Physics, Siberian Division, USSR Academy of Sciences,[116] which successfully combines the modulator and generator functions. In this device the spatial grouping of the beam is accomplished in a magnet placed between two undulators, with a high field of alternating polarity. This magnetic structure, which is similar to a single period of an undulator with $p_\perp^2 \gg 1$, provides the required modulation of the beam in a length substantially smaller than L_D.

The electromagnetic waves emitted by an electron in the first and second undulators of an optical klystron interfere, as a result of which a series of narrow spectral lines are observed in the direction of their common axis. The widths of these lines, which are determined by the relation of the phases of the interfering waves, are inversely proportional to the number of periods K_{0k} of electromagnetic oscillations which fit into the length of the wave pulse of light emitted in the optical klystron. Installation in the drift space of length d of a dispersing magnet with a field $p_{\perp d} = eH_m d / 2\pi mc^2 \gg 1$ permits substantial increase of the number K_{0k}:

$$K_{0k} = 2K + K_d, \quad K_d \approx \frac{d}{2\lambda\gamma^2}\left(1 + \frac{p_{\perp d}^2}{2}\right). \qquad (5.19)$$

The envelope of the spectral lines of the radiation in an optical klystron follows the shape of the spectral line of the radiation of a single undulator.

The dependence of the gain of a free electron laser on the energy spread can be reduced by using undulators with a transverse gradient of the magnetic field.[117] The distributions of the magnetic field strength and particle energy over the cross section of the beam are chosen so that particles with different energies emit radiation of the same wavelength; see Eq. (2.4).

In the weak-wave regime ($\Delta I \ll I$) the gain (5.17) does not depend on the intensity I. With increase of I the gain decreases (the saturation regime). For a wave intensity such that in the undulator length approximately half of the period of small phase oscillations occurs, the gain becomes mini-

mal. Here the efficiency of energy transfer (ET) of the beam to the wave becomes maximal. For undulators with constant parameters it is limited to a value $\Delta\gamma/\gamma \lesssim 1/K$. Actually, for $G > 0$ the energy of the beam particles decreases on passing through the undulator as the result of interaction with the electromagnetic wave. Accordingly the spectrum of spontaneous radiation of such particles in an undulator gradually shifts to the long-wave-length region. This shift decreases the detuning $\Delta\lambda = \lambda - \lambda_k$ with respect to the level of maximum gain (5.17), and when $\Delta\lambda$ changes sign the amplification of the wave is replaced by attenuation (absorption).

The energy transfer of a free electron laser can be raised substantially by using an undulator with parameters $p_{\perp 0}$ and λ_0 which vary along the undulator axis[117] in such a way that with decrease of the particle energy the condition of synchronism of the particle and the wave (5.15) is preserved (see Sec. 2).

To increase the efficiency of a free electron laser it is desirable to provide recovery of the processed electron beam[118] or to use multiple traversals of the beam through the undulator (for example, in electron storage rings[119,120]).

6. SOURCES OF UNDULATOR RADIATION IN SYNCHROTRONS AND STORAGE RINGS

6.1. Characteristics of operating synchrotron and storage rings. In contemporary electron synchrotrons and electron-positron storage rings, electron and positron beams with energies from tens of MeV up to tens of GeV circulate. These beams have high density, low emittance, and low energy spread, which makes them extremely suitable for production of undulator radiation.

The transverse size of the beam in an electron storage ring is determined mainly by synchrotron radiation.[81] The horizontal dimension of the beam is found from the condition of equilibrium between radiation damping (compression) of the beam and its pumping by quantum fluctuations of the synchrotron radiation. A typical value of the vertical emittance is about 10% of the horizontal emittance ($\varepsilon_y/\varepsilon_x = 0.1$).[94] The size of the beam and the angular spread of the particles in storage rings depend linearly on the energy of the particles.

The beam size $\sigma_{x,y}$ and its angular divergence $\sigma_{x',y'}$ at a given point of the orbit (at constant emittance) are determined by the magnetic structure of the storage ring, which in turn is characterized by the envelope of the betatron oscillations (the β function). In accordance with the requirements of an experiment, the β function at a given point of the orbit can be adjusted.[94] For placement of an undulator it is desirable to organize a portion of the orbit with a large value of the β function[17] and consequently with a small angular divergence of the beam. Another important characteristics of the magnetic structure is the dispersion function η, which determines the displacement of the particles when their momentum deviates from the equilibrium value. At the point of installation of an undulator it is desirable that this function take on its minimum value.[121]

6.2. Choice of parameters of the undulator radiation source. We mention at once that since the intensity of spontaneous undulator radiation is proportional to the beam current, it is quite obvious that the use of undulators in synchrotrons and storage rings is very promising since in these devices the electrons are used many times. In comparison with synchrotrons, storage rings have higher average values of the circulating current of particles and better beam quality.

Existing storage rings with energy E of the order of 1–10 GeV permit coverage of a broad region of the spectrum from visible radiation up to hard x rays. For generation of undulator radiation in the infrared region of the spectrum it is preferable to use undulators in low-energy continuous accelerators ($E \lesssim 0.1$ GeV) with high beam quality. Advance to the more energetic region of the spectrum (up to photon energies of the order of tens of MeV) is possible in electron storage rings with energy $E = 10$–50 GeV (Ref. 122) or in secondary electron beams obtained in very large proton accelerators.[93]

To obtain the greatest spectral density of radiation in the first harmonic it is desirable to choose fields in the undulator near the optimal value ($p_\perp \sim 1$).

If it is necessary to generate, in addition to the first harmonic, the first several harmonics of undulator radiation one should select a field amplitude corresponding to the transition region $p_\perp \gtrsim 1$. This condition will be optimal also for generation of coherent undulator radiation.[100] For generation of radiation of higher energy and greater power than ordinary synchrotron radiation one should use undulators with high fields or wigglers (see Sec. 4). In practically all cases precise tuning of the frequency of radiation can be accomplished by changing the amplitude of the magnetic field in the undulator.

Increase of the energy and intensity of undulator radiation for a given length of undulator can be accomplished by decreasing its period. For undulators with high fields ($p_\perp \gg 1$) the period is determined from considerations of obtaining the required value of magnetic field.

The width of the spectral line of undulator radiation and its intensity are given by the number of elements of periodicity of the undulator. With increase of the number of periods the width of the line will decrease, and the intensity will increase. However, increase of K above a certain value is not desirable since with further increase of K the influence of the particle beam parameters on the width of the spectral line and its intensity increases.

Optimal conditions for monochromatization of undulator radiation by diaphragming (5.5) are destroyed with increase of the particle energy as a consequence of the increase of directivity of the radiation ($\Delta\theta \sim \gamma^{-1}$) and increase of the angular spread of the beam ($\sigma_e \sim \gamma$). In storage rings in the portions of she orbit with low angular spread the required conditions for monochromatization are satisfied, as a rule, up to electron energies $E \lesssim 1$ GeV. In regard to synchrotrons, here the angular spread of the particles is greater than in storage rings, and therefore monochromatization conditions close to optimal can be achieved only at $E \lesssim 100$ MeV, i.e., in the optical wavelength region ($\lambda_0 \sim 3$–4 cm).

Since the emittance ϵ of a beam in an accelerator at a given energy is usually constant, in principle by appropriate adjustment of the magnetic system of the accelerator it is possible to select the optimal value of the angular spread, at which the spectral brightness [see Eq. (5.8)] will be greatest.[18] For an axially symmetric beam of particles under the condition

$$\varepsilon \gg \Delta\theta_{k0} d_k = \frac{\lambda_0}{2\gamma^2} \frac{1+(p_\perp^2/2)}{k} = \lambda_k \quad (\theta = 0)$$

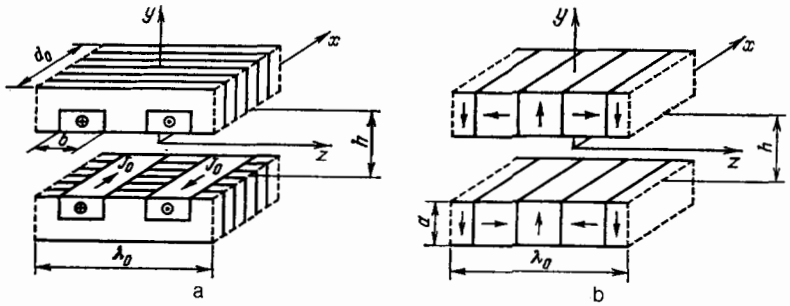

FIG. 10. Geometry of one period of an undulator. (a)–the electromagnetic undulator; the arrows show the direction of current in the winding (b)–permanent-magnet undulator; the arrows show the direction of the magnetic induction vector.

this spread is

$$\sigma_{x'm} = \sigma_{y'm} = \left(\frac{\sqrt{2}\,\varepsilon\Delta\theta_{k0}}{\pi L}\right)^{1/2}, \qquad (6.1)$$

and the maximum brightness is given by the expression[18,95]

$$B_m(\lambda,\ \theta=0) = \frac{\pi(\Delta\theta_{k0})^2}{\varepsilon^2}\frac{d^2 I_n}{d\lambda\, do}\quad(\lambda,\ \theta=0). \qquad (6.2)$$

Further increase of the spectral brightness requires decrease of the emittance of the particle beam.

6.3. The magnetic system of an undulator. An undulator is the main element of any source of undulator radiation. At the present time in UR sources two types of magnetic undulators are used: planar and helical. At the same time the search is continuing for methods of further improvement of the design of undulators and new types of apparatus are being developed which will permit substantial extension of their operational possibilities.

We shall consider the main features of the magnetic systems of various undulators and shall determine the relations for their parameters.

6.3.1. Planar undulator. The magnetic field of a planar undulator is created either by current-carrying coils (Fig. 10a) or by a system of permanent magnets (Fig. 10b).

In electromagnetic undulators the required magnetic field is excited by a system of parallel conductors oriented perpendicular to the undulator axis z and connected so that the direction of the current in neighboring wires is opposite. To increase the amplitude of the excited magnetic field, the conductors are placed in slots in magnetic yokes (see Fig. 10a).

The distribution of the transverse component of the magnetic field along the z axis in such an undulator depends in a rather complicated way on the geometry of the magnetic system, namely on the period of the structure λ_0, the gap h, and the conductor width b.[123,124] Numerical analysis shows that the amplitude of the magnetic field near the axis of the undulator rises rapidly with increase of the ratio of its period to the height of the magnetic gap and reaches a maximum value at $\lambda_0/h \approx 5$.[123,124] The form of this dependence for $h = 1$ cm is shown in Fig. 11, where H_m/J is the ratio of the field strength at the undulator axis to the value of the current in the windings. This dependence was calculated in the approximation of infinite magnetic permeability ($\mu \to \infty$) and infinitely thin wires ($b \to 0$). For a finite width of the conductors b the rise of the field strength with increase of λ_0/h occurs more smoothly. For a finite value of μ the amplitude of the field falls off slowly with increase of λ_0/h after reaching its maximum.

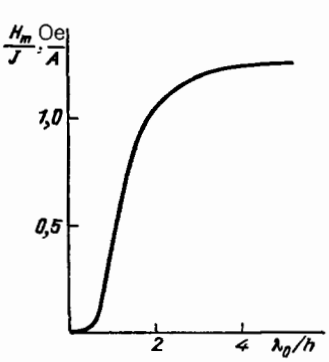

FIG. 11. Magnetic field amplitude as a function of undulator period with $h = 1$ cm.

For an undulator employing permanent magnets[125] the amplitude of the magnetic field can be represented in a comparatively simple analytic form[126]

$$H_m = 2H_c\frac{\sin(\pi/M)}{\pi/M}\left(1 - e^{-2\pi a/\lambda_0}\right)e^{-\pi h/\lambda_0}, \qquad (6.3)$$

where H_c is the coercive force, a is the height of the magnetic block, and M is the number of blocks in one period. The arrangement of magnetic blocks in a period of an undulator for $M = 4$ is shown in Fig. 10b. The nature of variation of the field amplitude with increase of λ_0/h is approximately the same as in an electromagnetic undulator.

It should be mentioned that in both versions for values $\lambda_0/h > 4$ the law of variation of the field along the undulator axis differs appreciably from sinusoidal.[123,127] Here the nature of the variation also will depend strongly on the number of magnetic blocks M and, in an electromagnetic undulator, on the conductor width b.

The inhomogeneity of the magnetic field in the gap of a planar undulator is determined mainly by the length of its period λ_0. If the width of the undulator is $d_0 > \lambda_0$, then according to Ref. 127 we have

$$\frac{1}{H_m}\frac{\partial^2 H_m}{\partial y^2} \approx \left(\frac{2\pi}{\lambda_0}\right)^2, \qquad (6.4)$$

from which it follows that the field inhomogeneity and consequently also the broadening of the spectral line of undulator radiation (5.6) fall off with increase of the undulator period.

Taking into account the form of the curve in Fig. 11, for obtaining a maximum value of $p_\perp \sim H_m\lambda_0$ for a fixed period the ratio λ_0/h must be chosen equal to 2–3. Here the shape of the distribution of the magnetic field is close to sinusoidal.

In the literature there is also discussion of periodic domain structures, which occupy a position intermediate between the macroscopic system discussed above and the atomic fields of crystals.[128] For example, in cobalt, where

$\lambda \lesssim 10^{-2}$ cm, the field reaches values $H_{ym} \sim 3$ kOe ($p_\perp \sim 3 \cdot 10^{-3}$).

6.3.2. Helical undulator. The design of a helical undulator has been discussed in Ref. 57. Such an undulator is a system consisting of two identical coaxial solenoids dislaced relative to each other by half of the winding pitch $\lambda_0/2$.

At one end the solenoid coils are connected in series, and the power supply is connected to the other end, which creates currents in the solenoids of opposite direction. With this commutation of the coils on the undulator axis a transverse helical magnetic field (3.8) is created, in which the direction of rotation of the vector coincides with the direction of the winding of the solenoids.

The amplitude of the magnetic field near the axis of such an undulator can be represented in the form[91]

$$H_R(\text{Oe}) = \frac{0{,}4J\,(\text{A})}{R_1} \frac{\sin \chi_0}{\chi_0} f(\alpha, \chi_1), \tag{6.5}$$

where

$$f(\alpha, \chi_1) = \frac{1}{\alpha}\left[K_0(\chi_1) - K_0(\chi_1(1+\alpha))\right] + \frac{\chi_1}{\alpha}\left[K_1(\chi_1) - (1+\alpha) K_1(\chi_1(1+\alpha))\right],$$

$$\alpha = \frac{R_2 - R_1}{R_1}, \quad \chi_0 = \frac{\pi b}{\lambda_0 \sin \psi}, \quad \chi_1 = \frac{2\pi R_1}{\lambda_0},$$

ψ is the angle of winding of the helix, $\operatorname{tg} \psi = \lambda_0/\pi(R_1 + R_2)$, R_1 and R_2 are respectively the inner and outer radii of the cylindrical coil ($R_2 - R_1 = d$, the thickness), b is the width of the conductor making up the coil, and K_0 and K_1 are Macdonald functions. We note that the expression (6.5) recalls expression (6.3) for the planar undulator.

The coefficient $\sin \chi_0/\chi_0$ characterizes the influence of the conductor width b on the magnetic field strength. Since b does not exceed $\lambda_0 \sin \psi/2$, this coefficient can change within the limits $2/\pi \leqslant \sin \chi_0/\chi_0 \leqslant 1$. The function $f(\alpha, \chi_1)$ expresses the dependence of the magnetic field amplitude on the conductor thickness d.

The amplitude of the field near the axis of a helical undulator reaches its maximum value at $\lambda_0/R_1 \sim 2\pi$. Here, as in a planar undulator, the lower value of the period is limited by the inner radius of the undulator. On departure from the undulator axis by a distance ΔR no greater than $0.1\lambda_0$ the expression (6.5) describes the magnetic field in the undulator with high accuracy (better than 1%).[76] For $\Delta R > 0.1\lambda_0$ the magnetic field strength increases rapidly with radius, and higher harmonics become appreciable in its distribution along the z axis. Here in motion along the undulator axis the tip of the vector will trace out not a circle, but an ellipse.

Therefore, for transverse beam dimensions appreciably greater than $0.1\lambda_0$, the radiation in the direction of the undulator axis will not be completely circularly polarized even in the case of a parallel beam. In addition, the inhomogeneity of the field over the cross section will lead to a broadening of the spectral line of undulator radiation (5.6), and in its spectrum, in addition to the fundamental, higher harmonics of the radiation will appear.

Permanent magnets can also be used in construction of a helical undulator.

6.3.3. A universal helical undulator. At the P. N. Lebedev Physics Institute a version of helical undulator[91,129] has been proposed and constructed which is called by the authors universal, in which the form of polarization of the electromagnetic radiation can be easily adjusted. This undulator consists of two concentrically placed simple helical undulators, one placed inside the other. The winding step is the same in the two undulators, and the direction of the winding is opposite. The power supplies of the two are independent.

Turning on only the outer winding or only the inner winding gives the direction of rotation of the magnetic field vector and correspondingly the polarization of the radiation (right-handed or left-handed).

The series connection of the two coils creates a magnetic field of the form (3.1) with $H_m = 2H_R$, whose vector will lie in a given plane. In this case the particles will move in a single plane according to a law (3.2) and consequently will emit linearly polarized radiation. A change of the direction of the current in one of the windings to the opposite leads to rotation of the field vector and correspondingly of the plane of polarization of the radiation by 90°.

Everything which has been said about the universal helical undulator applies to its radiation in the first harmonic. In Ref. 130 a modification of the design of the universal helical undulator was proposed which permits circularly polarized radiation to be obtained also in the higher harmonics.

6.3.4. Edge fields of an undulator. To exclude the influence of the undulator on the shape of the equilibrium orbit of the cyclic accelerator and to avoid distortion of the spectrum of undulator radiation it is necessary that the distribution of the magnetic field be antisymmetric with respect to the center of the undulator. Failure to observe this condition may be due to the presence of edge effects. If it is necessary the edge fields can be controlled either by correcting coils[131] or by changing the gap between the poles of the end blocks,[35] or finally by rotation of special edge magnetic blocks.[126]

It must be taken into account that the magnitude and shape of the edge field influence also the spectral characteristics of the radiation.

6.3.5. Undulators for free electron lasers. The gain of a free electron laser is proportional to the cube of the number of elements of periodicity of the undulator (5.17). The effective number of periodicity elements can be efficiently increased by using magnetic systems of the optical-klystron type. A modification of the optical klystron is being discussed in which the period of the second undulator is an integral number of times smaller than the period of the first undulator.[132] Such a system permits generation of coherent undulator radiation even in the higher harmonics.

In order to increase the efficiency of transfer of the energy of the particle beam to the electromagnetic wave, undulators are being constructed with parameters $\lambda_0(z)$ and $H_m(z)$ which vary monotonically along the undulator axis.[133,134] In such "variable" undulators a gradual change of the gap $h(z)$ between magnet poles is carried out along the beam path. The depth of modulation of the magnetic field $\delta_h = \Delta H_m/H_m$ in this case is determined by the magnitude of the change of the gap $\Delta H(z)$; see for example Eq. (6.3). Such systems permit increase of the efficiency of generation by several times. However, it must be kept in mind that with increase of the modulation depth δ_h there is a rise in the width of the spontaneous-radiation line and accordingly the starting current of the free electron laser increases. To decrease the starting current one uses a so-called multicomponent undulator consisting of several undulators with constant and variable parameters.[135]

TABLE II. Parameters of undulator radiation sources in synchrotrons and storage rings.

Sources of electrons				Undulators					Radiation		
Name, city, country	Type	E_m, GeV	J, A	λ_0, cm	K	H_m, kOe	$p_\perp$	Type	$\lambda_0/2\gamma^2$, Å	λ_{1m}, Å	$\Delta\lambda/\lambda_{1m}$
SOR–RING, Tokyo[36]	Storage ring	0,38		4	19	1,34	0,5	Planar, permanent magnets	350	405	0,047
ACO, Orsay, France[34]	»	0,56	0,1	4	23	5,1	1,9	Planar, superconducting electromagnet	166	765	0,039
Ref. 35	»	0,56	0,1	7,8	17	3,1	2,3	Planar, permanent magnets	323	1 177	0,053
VÉPP-2M, Novosibirsk, USSR[37]	»	0,67	0,1	2,4	10	1,3	0,4	Helical electromagnet	69	74	0,089
Ref. 149	»			2,4	8	4,7	1,5	Superconducting helical magnet	69	146	0,111
Pakhra, Moscow, USSR[22-26]	Synchrotron	1,2	0,03	4	20	1,9	0,7	Planar, electromagnet	36	45	0,045
Sirius, Tomsk, USSR[27-29]	»	1,5	0,03	14	5	1,5	2,0	Planar, electromagnet	81	243	0,178
ADONE, Frascati, Italy[33]	Storage ring	1,5	0,06	11,6	20	3,2	3,5	» »	67	477	0,045
VÉPP-3, Novosibirsk, USSR[30]	»	2,2	0,12	9	10	35	30	Planar, superconducting electromagnet	24	10 824	0,089
DORIS-II, Hamburg, West Germany[38]	»	3,7	0,06	13,2	16	6	7,4	Planar, permanent magnets	12	341	0,056
SSRL, Stanford, USA[31,32]	»	4,0	0,09	6,1	30	2,4	1,4	Planar, permanent magnets	5	10	0,030
Photon factory, Japan[37]	»	2,5	0,15	6	60	3,2	1,8	» »	12,5	32	0,015
VEPP-4, Novosibirsk, USSR[163]	»	8,5	0,02	22	5	16	32,9	Planar, electromagnet	4	2 147	0,178

6.4. Combination of an undulator with a cyclic accelerator. For installation of an undulator in the orbit it is necessary to have sufficiently long straight sections in the accelerator magnet.

The minimum height of the magnet gap of an undulator is given by the transverse size of the working region of the accelerator. The undulator gap can be reduced only in the case in which a previously well shaped particle beam is used for injection. If the electron beam is inadequately well shaped (which always occurs on injection of a low energy beam), the undulator can be placed beyond the working region and the beam of accelerated electrons at a given moment of time can be deflected by a special magnetic system from the equilibrium orbit and passed through the undulator. Here the minimum height of the gap is determined by the transverse size σ_y of the accelerated beam. In storage rings the height of the undulator gap must be matched to the specified lifetime of the beam.

6.4.1. An undulator for the Pakhra synchrotron. The Pakhra synchrotron has become the first cyclic accelerator from whose orbit undulator radiation has been obtained. It has a comparatively large working region ($\Delta x \cdot \Delta y = 15 \times 6$ cm^2). The angular spread and transverse dimensions of the accelerated electron beam in the energy range 100–700 MeV are $\sigma_x \lesssim 3$ mm, $\sigma_y \lesssim 2$ mm, $\sigma_{x'} \lesssim 0.45$ mrad, and $\sigma_{y'} \lesssim 0.35$ mrad, respectively. The repetition frequency of the magnetic field cycles is $f = 50$ Hz.

For these dimensions of the working region of the accelerator the placement in its equilibrium orbit of a planar (symmetric) undulator with a small period ($\lambda_0 < 6$ cm) would sharply reduce the intensity of the accelerated beam as a result of the diaphragming action of the undulator. Therefore an asymmetric undulator was used, which consists only of one half which was placed at the limit of the working region somewhat above the median plane. The accelerated electrons were brought up to it to a distance $y \sim 1.5$ cm by the radial component of the magnetic field, which is produced by the undulator itself. The magnitude of this displacement was controlled by means of a small change of the gradient of the guiding field of the synchrotron. Such an undulator is equivalent in its properties to a symmetric undulator with $h = 2y$.[123]

The undulator is made in the form of a ferromagnetic comb with current-carrying wires placed in its slots and oriented perpendicular to the electron-beam axis. The undulator period λ_0 was chosen as 4 cm. A similar symmetric undulator with period about 3 mm has been developed in Ref. 36 with application to free electron lasers.

The power supply for the undulator winding is pulsed. The maximum amplitude of the current is $J = 8$ kA, the duration of the flat top of the pulse is 2 msec, and the repetition frequency is 50 Hz. The current $J = 8$ kA and the distance to the undulator plane ~ 1 cm correspond to a value $p_\perp = 0.7$.

6.4.2. Sources of undulator radiation in synchrotrons and storage rings. In Table II below we have given the main parameters of operating accelerators (or storage rings) and undulators, and also the characteristics of the undulator radiation obtained with them.

As follows from the table, the existing sources of UR (in the regime of low and optimal fields in the undulator, $p_\perp \lesssim 1$) cover a broad spectral range of frequencies from optical to soft x-rays. The undulators with high fields given in the table are intended for use in the shorter-wavelength region. The total radiation power of such sources ($p_\perp \gg 1$) at the present time has been raised to several kilowatts.[30] However, in a number of cases as the result of the necessity of using monochromators, only part of this power is utilized. In recent papers[31-37,137] it is shown that by using an undulator with fields close to optimal it is possible to create a radiation source in which practically all of the useful power is concentrated in a specified interval of the spectrum.

We note that of the thirteen undulators listed in the table, eleven are planar, and among them designs with permanent magnets are dominant. Helical undulators are less common. However, as a result of the possibility of obtaining with them circularly polarized radiation it is to be expected that the number of such devices will rise in the near future.

The undulators listed in Table II in the storage rings ACO (France) and ADONE (Italy) are used in a program of creating shortwavelength free electron lasers.[33,138] For the same purposes the optical klystron[139] was developed in Novosibirsk. It should be mentioned that the reliability of operation of such generators will depend on the quality of the mirrors, including their stability to the action of the energetic part of the spectrum of spontaneous undulator radiation and synchrotron radiation, which limits the operation of free electron lasers to the region of relatively low electron energies and fields in the undulator close to the optimal $p_\perp \sim 1$.[138]

7. EXPERIMENTAL STUDIES OF THE PROPERTIES OF UNDULATOR RADIATION

Study of the properties of undulator radiation and measurements utilizing it differ substantially from measurements carried out with ordinary light sources. The limited accessibility to the experimental apparatus requires careful and reliable preliminary adjustment of the optical elements of the measuring systems with respect to the radiation beam. The regime of operation of the accelerator or storage ring (particle energy, beam emittance, and so forth) is established taking into account the specified spectral range, the intensities required, and the time characteristics of the radiation. The time structure of a pulse of undulator radiation is determined by the mode of operation of the undulator and by the number of bunches in the orbit.

In setting up an experiment it is necessary to take into account that in the direction of the undulator axis in addition to undulator radiation there is propagated also the radiation of electrons from the edge fields of the bending magnets of the synchrotron or storage ring, which forms a background [22,140-144]

7.1. Spectral and angular characteristics. In the optical region of the spectrum the spectral and angular characteristics of the radiation have been recorded in the focal plane of an objective placed in the UR beam. This arrangement of the experiment permitted exclusion of the influence of the electron beam size on the results of the measurements.

A convenient representation of the spectral and angular distributions of undulator radiation are given by colored photographs. In them the image of the undulator radiation appears as a series of concentric colored arcs which together recall a rainbow, in which with increase of the radius of arc the wavelength of the radiation increases.

Experiments carried out using the Pakhra synchrotron

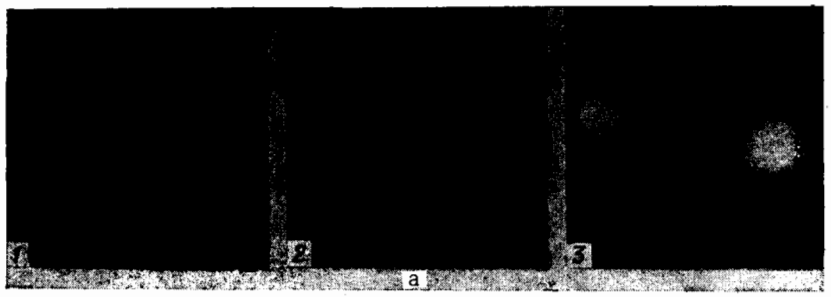

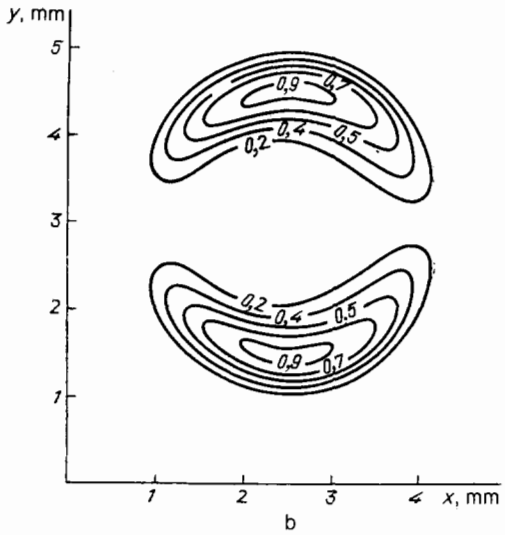

FIG. 12. (a)–Photographs of the first harmonic of undulator radiation at wavelength $\lambda_f = 3850$ Å for various electron energies E in MeV = 116 (1), 137 (2), and 194 (3).[23,26] (b)–Spatial distribution of undulator radiation for $E = 158$ MeV, $\lambda_f = 3850$ Å; scale: 1 mm corresponds to an angular interval 0.5 mrad.[24]

with a fixed wavelength (the wavelength $\lambda_f = 3850$ Å was separated by an ultraviolet optical filter with a relative transmission band $\Delta\lambda/\lambda_f = 4.4\%$) show that the form of the angular distributions changes substantially with the electron energy.[22-24,26] Here, as in other experiments in the Pakhra synchrotron, the value of the undulator field parameter is $p_\perp = 0.1$, which corresponds to dipole radiation. Monochromaticity of the radiating electrons was achieved by an appropriately timed turning off of the high-frequency voltage in the accelerating resonator of the synchrotron. For an electron energy close to the threshold $E_{thr} = 116$ MeV ($\lambda_{min} = \lambda_f$) a symmetric spot appears, which is shown in photograph 1 of Fig. 12a. With increase of the energy, at first the size of this spot increases while the shape is preserved. On further increase of the energy the central part of the spot disappears, and in the photographs (Fig. 12a) ring-shaped regions appear whose radius increases and whose width decreases; the radiation is being concentrated near the surface of the cone (4.8), the opening angle of which increases with energy. The general nature of the spatial distribution of the radiation (in the cross section) is shown in Fig. 12b for $E = 158$ MeV. Here the solid lines show levels of identical intensity. This figure proves that the radiation of the first harmonic is concentrated in two regions which have in their cross section the shape of a kidney bean and are symmetrically oriented with respect to the horizontal plane; this agrees with the conclusion mentioned above (see Sec. 4) regarding the azimuthal dependence of the angular distribution of undulator radiation emitted in a planar undulator. Under the conditions of the experiment the plane of oscillations of the particles in the undulator was oriented horizontally, and accordingly the maximum of the undulator radiation intensity lies in the vertical plane.

The dependence on the wavelength of the form of the angular distribution of the radiation in a distinguished plane was investigated in Ref. 25 by means of a spectrograph, and in Ref. 38 by means of a monochromator. The entrance slit of the spectral device was oriented perpendicular to the plane of oscillations of the particles in the undulator.

For the case of nondipole radiation ($p_\perp = 3.5$) the angular distributions of the first harmonic of the undulator radiation for various wavelengths (5200 Å$\leqslant\lambda\leqslant$6400 Å) were obtained in the storage ring ADONE ($E = 625$ MeV, $\lambda_0 = 11.6$ cm). The radiation beam was scanned in the plane of electron oscillations ($\varphi = 0,\pi$) by a monochromator placed at a distance 24 m from the center of the undulator (Fig. 13).[33] The figure shows that at $\theta = 0$ the maximum of the radiation occurs at a wavelength $\lambda = 5200$ Å, which is about seven times greater than the wavelength of dipole radiation ($\lambda_{1m} = \lambda_0/2\gamma^2$). It can also be seen that, as in the dipole case, with increase of the wavelength two maxima appear in the distribution of the undulator radiation, the distance between which gradually increases.

The influence of the electron-beam parameters on the spectral and angular characteristics of undulator radiation has been investigated in detail in the Pakhra synchrotron.[96,97] The results obtained in these experiments are shown in Fig. 14. The points refer to the angular distribution

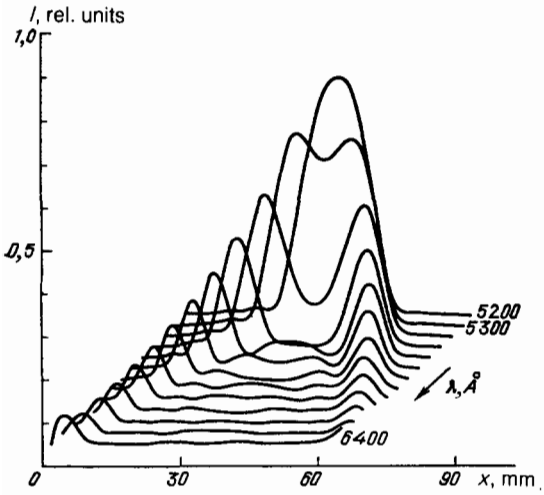

FIG. 13. Spectral and angular distribution of the first harmonic of undulator radiation ($\varphi = 0, \pi$).[33] $E = 625$ MeV. 1 cm corresponds to about 0.42 mrad.

of the intensity of radiation of the first harmonic in the vertical half-plane ($\varphi = \pi/2$) obtained by means of an ultraviolet optical filter ($\lambda_f = 1.37\lambda_m$) at an electron energy $E = 135.6$ MeV. The location of the maximum of the distribution determines the opening angle of the cone of undulator radiation with an error no greater than 5%. In the same figure we have shown the angular distribution calculated for similar conditions for a parallel beam (the narrow dashed curve). As can be seen, the observed distribution is about three times broader than the calculated one, which is due mainly to the angular spread of the particles in the beam.

Calculations were made with various values of the angular spread of the electron beam. Since the distribution of particles in the Pakhra synchrotron is close to axially symmetric, it can be described by a single parameter σ_e (5.2).[96,97] The best agreement with the experimental data was obtained with a dispersion value $\sigma_e^2 = 0.194$ mrad)^2 ($\sigma_e\gamma = 2.4/K$, the crosses on the curve in Fig. 14). The angular dispersion found in this way agrees rather well with the data of optical measurements on synchrotron radiation.[145]

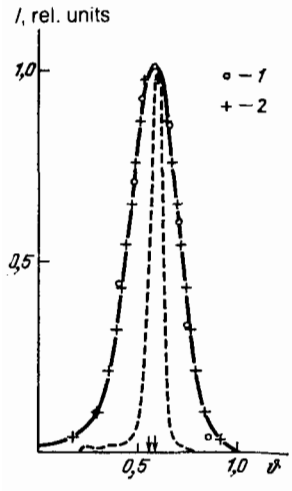

FIG. 14. Angular distribution of undulator radiation ($\varphi = \pi/2$) for $E = 136.6$ MeV, $\lambda_f = 3850$ Å. 1–Experiment, dashed curve–calculation for a parallel beam, 2–calculation for a beam with an axially symmetric angular distribution ($\sigma_e = 0.44$ mrad).[96,97]

The curves in Fig. 14 have been normalized to unity at the maximum. It follows from this that undulators with a large number of periodicity elements ($K \gtrsim 20$) can be used for measurements of the angular spread of the charged-particle beams in cyclic accelerators and storage rings.[97,146]

Also in this experiment a displacement of the maximum of the angular distribution of undulator radiation in the direction of smaller angles θ by an amount $\Delta\theta_m\gamma \sim 0.02$ was observed with respect to the angle θ_m (4.8), which is in good agreement with the estimates given in Sec. 5. The angular resolution was about 10^{-7} sr.

It should be mentioned that the comparatively small period of the undulator ($\lambda_0 = 4$ cm) permitted all measurements to be made with low background interference from synchrotron radiation. We point out, for example, that at an electron energy $E = 100$–160 MeV the intensity of undulator radiation in the ultraviolet region of the spectrum exceeds the intensity of synchrotron radiation by more than an order of magnitude. With further increase of the electron energy ($E > 160$ MeV) the time-averaged energy of synchrotron radiation at wavelength λ_f becomes comparable with the energy in the pulse of undulator radiation (of duration $\tau \sim 0.1$ msec) and then two side peaks, easily visible in the photograph (Fig. 12a), appear, which correspond to synchrotron radiation from the near and far quadrants of the accelerator. All of this clearly demonstrates the difference between undulator radiation and synchrotron radiation.

The features noted above of the angular distribution of undulator radiation have been observed also in other experiemnts. For example, in the Sirius synchrotron[28] in addition to measurements of the angular distributions of the first harmonic (for $\lambda_f = 5000$ Å, $p_\perp = 0.52$, $K = 5$) for various energy values ($\gamma_1 = 398.6$ and $\gamma_2 = \sqrt{2}\gamma_1$) the distribution of undulator radiation was observed for the first time in the higher harmonics.

In the storage rings SOR-RING[36,37] and VÉPP-2M[137] measurements have been made of the spectral and angular distribution of the intensity of undulator radiation in the soft-x-ray region and in the vacuum ultraviolet region.

References 36 and 37 have investigated the dependence of the wavelength λ_{1m} corresponding to the maximum in the spectrum of the first harmonic on the angle of observation, the undulator field parameter, and the electron energy. Each of the dependences obtained of λ_{1m} on ϑ^2, $p_\perp^2$, and γ^{-2} has a linear nature, which is in good agreement with Eq. (4.5). The influence of the emittance of the electron beam in these experiments appeared in a small shift ($\sim 2\%$) of λ_{1m} toward the long-wavelength region.

7.2. Polarization properties. The peculiar polarization characteristics of the radiation of electrons in a planar undulator have been investigated in the optical wavelength region.

Photographs of the distribution of the parallel and perpendicular components of the polarization of the first harmonic of undulator radiation obtained by means of Polaroid film in the Pakhra synchrotron[23] ($\vartheta_m = 1$), are shown in Fig. 15. The parallel component of the undulator radiation (Fig. 15a) has two maxima located near the vertical plane (a dipole distribution), while in the angular distribution of the perpendicular component of the undulator radiation (Fig. 15b) four symmetric maxima are distinguished (a quadrupole distribution).

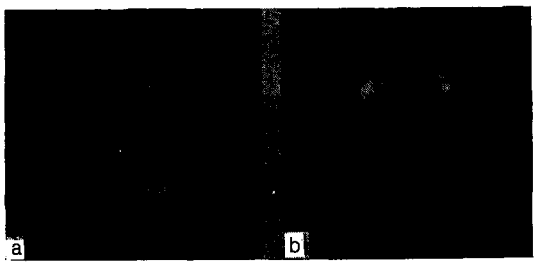

FIG. 15. Angular distribution of polarization of the first harmonic of undulator radiation: $E = 163$ MeV, $\lambda = 3850$ Å.[23] (a)–$\parallel$ component, (b)–$\perp$ component.

It can be seen that the observed pattern of the angular distribution in the first harmonic of undulator radiation is identical to the theoretically expected instantaneous angular distribution of undulator radiation.

The angular distribution of the polarization components of the harmonics of undulator radiation with $p_\perp = 1.1$ has been observed in the Sirius synchrotron.[29] It was shown that the distribution of the polarization components of the first harmonic ($E = 473$ MeV, $\lambda_f = 5000$ Å, $\vartheta = 1.74$) has the same properties as in the dipole case ($p_\perp \ll 1$). At lower electron energies ($E = 162$–215 MeV) radiation of the second harmonic appears. In the angular distribution of its parallel component two maxima are observed, while in the distribution of the perpendicular component there are six. The existence of an even number of maxima in the azimuthal distribution of the two components of the radiation is characteristic also for higher harmonics (see Sec. 4). We note that these angular distributions of the radiation recall the configuration of the transverse modes of gas-discharge lasers (see for example Ref. 147).

In Ref. 148 spectra were measured of the polarization components of the first harmonic of undulator radiation ($p_\perp = 1.05$). It was shown that the spectrum of the parallel component is close in shape to the total spectrum of the radiation. The spectrum of the perpendicular component is a smooth curve with a small maximum lying at

$$\frac{\lambda}{\lambda_m}\left(1 + \frac{p_\perp^2}{2}\right) \sim 0{,}3.$$

The ratio of the maxima of the spectra of these components is about 5.7.

An experimental study of the polarization characteristics of the radiation from electrons in a helical undulator has been carried out in the VÉPP-2M storage ring in the soft x-ray region,[149] The results of the measurements indicate a high degree of circular polarization of the undulator radiation.

7.3. Spectral distribution. Undulator radiation has the characteristic feature that its spectral properties depend on the angle of observation. The spectrum of radiation propagated along the undulator axis where the intensity of the radiation is greatest has been studied in Refs. 25, 26, 28–37, and 137. A circular diaphragm placed on the extension of the undulator axis was used.

In Refs. 25 and 26, in which studies were carried out at an electron energy $E = 143.3$ MeV, the angular size of the diaphragm was optimal (5.5) and amounted to $\Delta\theta_d = 0.8$ mrad ($\Delta\vartheta_d = K^{-1/2} = 0.22$). The experimental results obtained are given in Fig. 16, where they are shown by circles.

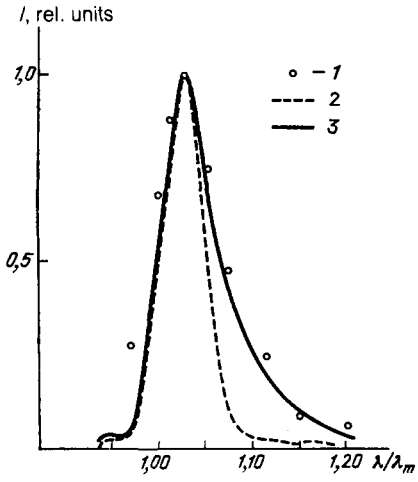

FIG. 16. Spectral distribution of the first harmonic of undulator radiation for $E = 143.3$ MeV, $\Delta\vartheta_d = 0.225$. Curve 1–experiment, curve 2–calculation for a parallel beam, curve 3–calculation for a beam with $\sigma_e = 0.44$ mrad.

The results of a theoretical calculation carried out for a parallel electron beam are shown in this same figure by the dashed curve. To the right of the maximum the experimental points deviate from this curve in the direction of longer wavelengths. In the calculations corrections were made for the angular spread of the electron beam ($\sigma_e = 0.44$ mrad). When these corrections are taken into account, the dashed curve is converted into the solid curve, which is in good agreement with the experimental data. The half-width of the measured spectrum is about 8%, while for the parallel beam it would be 5%. The maximum of the spectral distribution occurs at a wavelength $\lambda = 2610$ Å. For an infinitely small diaphragm ($\Delta\vartheta_d \ll K^{-1/2}$) this maximum should occur at a wavelength $\lambda_m = 2534$ Å. The shift of the maximum is due to the finite size of the diaphragm used. In the experiments described an ISP-28 spectrograph was used. The location of the maximum of the spectrum was measured with an accuracy of about 1%. Measurements made for a fixed electron energy by means of ordinary spectral instruments permitted the shape of the spectral distribution of the radiation to be determined with high accuracy.

References 28 and 29 used a method of measurement of the spectral distribution based on the universal dependence of the spectrum on the quantity $u = 2\gamma^2\lambda/\lambda_0$. A wide range of variation of u for a fixed wavelength $\lambda_f = 5000$ Å was achieved by changing the electron energy. However, it should be mentioned that such measurements require introduction of corrections taking into account the dependence on the electron energy of the angular spread of the beam and of the fraction of the radiation transmitted by the diaphragm (5.4), and this is not always easy to carry out.

In these experiments it was found that, in accordance with the theory,[17,57] the greatest amplitude of the spectrum is observed for $p_\perp = 1.1$–1.3 (the optimal field of the undulator). Here it was observed also that the spectral line is broadened in the long-wavelength direction as the result of the influence of the angular spread of the particles in the beam. The angular size of the diaphragm was $\Delta\vartheta_d \ll K^{-1/2}$.

In electron storage rings measurements of the spectral distribution of undulator radiation in the optical wavelength

range have been made in Refs. 30–33 and 35 at comparatively low electron energies. As a consequence of the small angular divergence of the electron beam the line widths measured in these experiments turned out to be close to the values expected theoretically for parallel beams.

On increase of the electron energy the radiation spectrum shifts toward the vacuum ultraviolet region. As a consequence of the increase in directivity of the radiation and the increase of the angular spread of the beam, in measurements of the profile of the spectral line of the first harmonic some deviation is observed from a calculation carried out in the single-particle approximation.[36–38]

Measurements of the absolute spectral intensity of undulator radiation in the soft-x-ray region and in the vacuum ultraviolet region by means of ionization chambers filled with an inert gas have been made at the VÉPP-2M storage ring[137] and at the Photon Factory in Japan.[36,37] In Ref. 36 with an undulator field $p_\perp = 0.47$ and $\gamma = 743.6$ ($\lambda_0 = 4$ cm, $K = 19$) the flux of photons with wavelength $\lambda = 400$ Å turned out to be $N_\lambda = 6.6 \cdot 10^{11}$ photons/sec·mA·mrad^2 ·1%. Approximately the same photon flux was obtained in Ref. 137 at a wavelength $\lambda = 133$ Å with $p_\perp = 0.24$ and $\gamma = 998$ ($\lambda_0 = 2.4$ cm, $K = 10$). A significantly higher spectral density of radiation $N_\lambda \lesssim 10^{14}$ photons/sec·mA·mrad^2 ·1% was obtained in Ref. 37 at a wavelength $\lambda \sim 28$ Å ($\hbar\omega \sim 450$ eV) in an undulator with $\lambda_0 = 6$ cm, $K = 60$, $p_\perp \approx 1$ with $\gamma = 4900$. We note that this value would be about two orders of magnitude higher if the beam had negligible emittance.

Thus, the radiation intensity obtained in an undulator is one to two orders of magnitude higher than the corresponding intensity of synchrotron radiation obtained in similar installations (see for example Ref. 5).

In the ideal case (in the absence of angular spread in the beam) in the direction of the electron beam in a planar undulator the observer is dealing only with odd harmonics. When there is some angular spread in the beam, even harmonics can also be radiated along the undulator axis, and this was observed in the studies mentioned above[29,36,137] (the second harmonic).

The spectral distribution of the total (integrated over all angles) intensity of undulator radiation was investigated in Refs. 27 and 148 for fields close to optimal. The observed distribution is extremely close in shape to the calculated curves shown in Fig. 7a. The difference reduces mainly to the smoothed shape of the peaks, which is due to the finite length of the undulator, which in the experiments being discussed had only five periodicity elements. The shape of the integrated spectrum of undulator radiation in the x-ray region ($\hbar\omega = 1$–7 keV) with $p_\perp = 0.3$–1.35 and $E = 3$ GeV and in the vacuum ultraviolet region ($\hbar\omega = 20$–200 eV) with $p_\perp = 6.41$ and $E = 3.7$ GeV was measured in Ref. 32, where a quasi-line nature of the radiation spectrum was also observed.

Summing up, it is interesting to note that the shape of the integrated radiation spectrum observed in experiments in undulators has much in common with the radiation spectra of ultrarelativistic positrons occurring during channeling in crystals.[70,71,150,151] The amplitude of the first harmonic of the radiation at some (optimal) particle energy reaches a maximum value.[151] This also is to be expected since in both cases we are dealing with the periodic motion of fast charged particles.[57]

7.4. Spatial coherence of undulator radiation. The waves at the output of an undulator have the property of spatial coherence. This phenomenon was pointed out for the first time in Ref. 104.

A subsequent experimental confirmation was made in the VÉPP-2M storage ring.[137] In that work at wavelength $\lambda = 130$ Å at electron energy $E = 0.51$ GeV with transverse beam dimensions $\sim 0.06 \times 0.02$ cm the authors observed interference of undulator radiation passing through two apertures of diameter $\sim 6\,\mu$m in a silicon membrane of thickness about $2\,\mu$m. The membrane was placed a distance 520 cm from the undulator. These experiments determined the angle $\theta_{\rm coh}$ which limits the region of spatial coherence of undulator radiation, and which turned out to be in good agreement with the value determined by Eq. (5.14).

7.5. Coherent undulator radiation. At the present time in a number of laboratories work is being carried out on construction of generators of coherent undulator radiation in the optical region (free electron lasers). The results of these studies are partially reflected in the preceding paragraphs of the present section.

In Ref. 139 the properties of spontaneous radiation in an optical klystron were studied. Here each of the two undulators of the optical klystron had three periods of length 10 cm each, and the amplitude of the magnetic field of each of the undulators was $H_m \approx 3$ kOe ($p_\perp = 2.8$). The dispersive section had a length $d = 34$ cm, and the magnetic field in it was $H_d \approx 5.7$ kOe ($p_{\perp d} = 19.5$).

Using this optical klystron spontaneous radiation lying in the visible region was obtained. A portion of the spectrum measured at electron energy $E = 350$ MeV is shown in Fig. 17a. The spectrum consists of narrow spectral lines with a relative width of each line $\Delta\lambda/\lambda \sim 1/170$, which is in satisfactory agreement with estimates of the effective number of periods of such an optical klystron (5.20) $K_{\rm OK} \approx 150$.

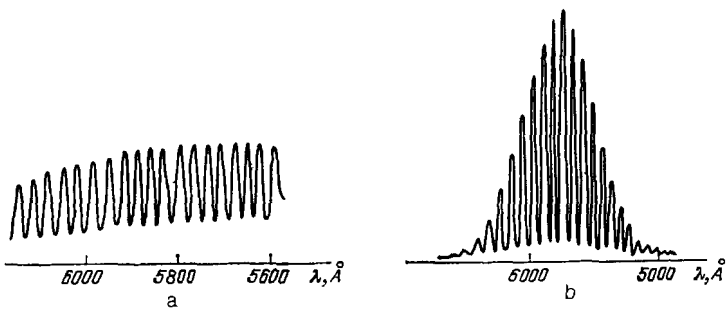

FIG. 17. Portion of spectrum of spontaneous radiation of electrons in an optical klystron. (a)–$E = 350$ MeV.[139] (b)–$E = 240$ MeV.[138]

In order to improve the characteristics of the radiation, in the same laboratory a new optical klystron was constructed[152] (sic) with an effective number of periodicity elements $K_{OK} \approx 290$.

The measured gain was 1.5%. In ordinary undulators in storage rings the gain[33,35] is of the order of several units times 10^{-4},

Generation of coherent undulator radiation has been obtained by means of an optical klystron in the ACO storage ring.[138] The optical klystron was constructed by replacing the three central periods by a three-pole dispersive section in an undulator consisting of 17 elements of periodicity (see Table II). The number K_d [see Eq. (5.20)] was determined from measurements of the spectrum of spontaneous undulator radiation. At an electron energy $E = 240$ MeV and $p_\perp = 2.1$ it turned out to be 65 (see Fig. 17b), while the theory predicts a value $K_d = 68$.[35] The width of the spectrum envelope corresponds to $K = 8.1$. With decrease of the electron energy and a corresponding decrease of the undulator field required for preservation of the wavelength ($\lambda = 6328$ Å) the value of K_d increases [see Eq. (5.20)] and at $E = 150$ MeV it is $K_d = 84$.

In the generation mode a resonator was used which had a length of 5.6 m and consisted of two spherical mirrors with radii of curvature 3 m and reflection coefficient in the wavelength range 6200–6800 Å equal to 99.965%. Maximum generation was obtained at a wavelength $\lambda \sim 6500$ Å (the portion of maximum steepness of the spontaneous radiation spectrum; see Sec. 5).[138] For an electron energy $E = 166$ MeV, $p_\perp = 1.1$–1.2, and a beam current $J = 50$ mA, the average power of the extracted coherent radiation was about 75 μW, which corresponds to about 60 mW in a pulse of duration of the order of 1 nsec. The pulsed power stored in the resonator was ~ 2 kW. It is interesting to note that the average power of the coherent radiation is $2.4 \cdot 10^{-5}$ of the total power of synchrotron radiation of an electron beam of the same energy and current.

In addition to constructing optical generators of coherent undulator radiation in storage rings, active searches are being carried out for methods of increasing the efficiency of free electron lasers employing linear electron accelerators.[49,133–135] Recently at Stanford in the superconducting linear accelerator (electron energy $E = 66$ MeV, beam current $J = 0.5$–2.5 A, energy spread $\Delta\gamma/\gamma \sim 0.03\%$, emittance $\sim 0.15\pi$ mm·mrad) generation of coherent undulator radiation was obtained at a wavelength $\lambda = 1.57$ μm.[135] This work utilized a multicomponent undulator consisting of two ordinary undulators ($K = 5\ 1/2 + 15$) located at the ends of the generator and a main variable (tapered) undulator (wiggler) ($K = 90$) placed after the dispersion section in front of the last undulator (see Sec. 6). The undulator is made up of $SmCo_5$ permanent magnets and has a period $\lambda_0 = 3.6$ cm and a total number of periodicity elements $K = 131$. The maximim value of the field is $H_m = 2.9$ kOe ($p_\perp \approx 0.98$). The decrease of the magnetic field H_m of the variable undulator is achieved by gradual increase of its gap. In the experiments described the maximum value of δ_h at the undulator exit was 0.02.

The shape of the spontaneous-radiation spectral line was investigated. For $\delta_h = 0.01$ the line width at half-height was $\Delta\lambda/\lambda \sim 3\%$, which is more than three times the value of $1/K$. The line has an asymmetric shape recalling the curves shown in Fig. 16 (see also Ref. 152).

The lasing mode utilized an optical resonator of length 12.68 m consisting of spherical mirrors with radii of curvature 7.5 m and reflection coefficient at wavelength $\lambda = 1.6$ μm equal to 99.84%. For $\delta_h \sim 0.01$–0.02 the lasing efficiency was increased substantially in this experiment, from $\eta = 0.4\%$ at $\delta_h = 0$ up to $\eta = 1.1$–1.2%. In addition to the first harmonic, in these experiments lasing was also observed at the second harmonic (0.8 μm) and the third harmonic (0.52 μm). A gain of about 7% per pass was obtained in a regime far from saturation.

Lasing in the far infrared region of the spectrum ($\lambda = 400$ μm) was obtained in a free electron laser with reestablishment (recuperation) of the energy ($\gtrsim 90\%$) of the electron beam.[153] The source of electrons was a Van de Graaff electrostatic accelerator of energy 3 MeV. An undulator employing permanent magnets with a period $\lambda_0 = 3.6$ cm and a total length $L = 715$ cm was used. The field on the undulator axis was $H_m = 460$ Oe. A peak radiation power of 10 kW in a pulse of duration 50 μsec was achieved.

7.6. Undulator radiation from protons and antiprotons. Recently in connection with the construction of proton accelerators of superhigh energy (hundreds of GeV) it has been found that for determination of the important geometrical parameters of the beams it is possible to use the synchrotron radiation of protons. It is obvious that the use of synchrotron radiation is not very efficient here, since even at such high energies it lies in the far infrared region where detection of the radiation is extremely difficult.

However, by using an undulator it is possible to obtain proton radiation lying in a shorter-wavelength region which is more easily measured.[154,155] This was first accomplished in the proton and antiproton beams of the CERN collider.[156] The planar magnetic undulator used for this purpose had the following parameters: maximum magnetic field $H_m \approx 3.6$ kOe, period $\lambda_0 = 8.8$ cm, number of periods $K = 5$. The field parameter of this undulator for protons was $p_\perp \approx 1.6 \cdot 10^{-3}$.

The rather high intensity of undulator radiation of the proton beams ($N_p = 5 \cdot 10^{11}$) and of the antiproton beams $N_{\bar{p}} = 5 \cdot 10^9$) with energy 270 GeV made it possible to measure the profile of the particle beams with a spatial resolution ~ 0.1–0.2 nm for characteristic beam dimensions 2–3 mm. In the work discussed, concurrent measurements were made of the spectral and angular characteristics of the proton radiation in the wavelength range $\lambda = 5000$–6000 Å. As expected, the results turned out to be in good agreement with the results of theoretical calculations.

8. CONCLUSIONS

At the present time sources of undulator radiation are finding practical application in investigations in the vacuum ultraviolet and more energetic regions of the spectrum where there is perceived to be a lack of intense tunable sources of electromagnetic radiation. Already there are interesting results of use of such sources in studies of x-ray fluorescence elemental analysis, nuclear spectroscopy, medical diagnostics, and vacuum ultraviolet spectroscopy.[157,158]

There is no doubt that in the near future the use of such sources will become more extensive. For example, in all plans for specialized sources of synchrotron radiation which

are being carried out or developed at the present time, the undulator is becoming an important element. The existence in the very large proton synchrotrons of intense beams of monoenergetic electrons of high energy (tens and hundreds of GeV) and the construction in the not too distant future of colliding electron-positron beams with energy up to 100 GeV will permit the generation, by slowing down such beams in an undulator, of intense fluxes of polarized quasi-monochromatic photons of high energy (of the order of several MeV and above; see Table II).[93,122,159] Such photons present independent interest for production of polarized electrons and positrons in linear colliding electron-positron beams (VLÉPP)[159,160] and for studies in she fields of photonuclear physics and high-energy physics.

By use of the radiation of a helical undulator installed in an electron-positron collider it is is possible to obtain fluxes of monochromatic circularly polarized photons which arise in Compton scattering of the undulator radiation of one of the beams by the other colliding beam.[161] The energies of such photons will be close to the energy of the colliding particles. On the basis of their angular distribution it is possible to deduce the polarization of the electron-positron beams.[162]

In conclusion the authors consider it a pleasant duty to express their gratitude to K. A. Belovintsev, E. G. Bessonov, B. M. Bolotovskiĭ, and V. L. Ginzburg, who examined the manuscript and made valuable remarks.

[1]*Synchrotron Radiation in Solid State Research* (in Russian), a collection of articles, Mir, M., 1970.
[2]R. P. Godwin, *Synchrotron Radiation as a Light Source*, Springer Tracts in Modern Physics, Vol. 51, Springer-Verlag, Berlin-Heidelberg-New York, 1969. [Russ. transl. Usp. Fiz. Nauk **101**, 493 (1970)].
[3]M. N. Yakimenko, Usp. Fiz. Nauk **114**, 55 (1974) [Sov. Phys. Uspekhi **17**, 651 (1975)].
[4]S. P. Kapitsa, Vestnik AN SSSR, No. 8, 28 (1975).
[5]G. N. Kulipanov and A. N. Skrinskiĭ, Usp. Fiz. Nauk **22**, 369 (1977) [Sov. Phys. Usp. **20**, 559 (1977)].
[6]Synchrotron Radiation Research, Ed. by H. Winick and S. Doniach, Plenum, New York, London, 1980.
[7]*Synchrotron Radiation: Properties and Applications.* A collection of articles edited by K. Kunz (translated from German), Mir, M., 1981.
[8]I. M. Ternov and V. V. Mikhaĭlin, *Synchrotron Radiation: Theory and Experiment* (in Russian), Énergoatomizdat, M., 1986.
[9]V. L.Ginzburg, Izv. AN SSSR, Ser. Fiz. **11**, 165 (1947).
[10]H. Motz, J. Appl. Phys. **22**, 547 (1951); [Russ. transl. in Ref. 12, p. 194].
[11]H. Motz, W. Thon, and R. N. Whitehurst, J. Appl. Phys. **24**, 856 (1953); [Russ. transl. in Ref. 12, p. 317].
[12]*Millimeter and submillimeter waves* (in Russian), A collection of articles, translated from English, IL, M., 1959.
[13]I. A. Grishaev, V. I. Myakota, V. I. Kolosov, *et al.*, Dokl. Akad. Nauk SSSR **131**, 61 (1960) [Sov. Phys. Dokl. **5**, 272 (1960)].
[14]A. I. Alikhanyan, S. K. Esin, K. A. Isparyan, *et al.*, Pis'ma Zh. Eksp. Teor. Fiz. **15**, 142 (1972) [JETP. Lett. **15**, 98 (1972)].
[15]D. F. Alferov, Yu. A. Bashmakov, and E. G. Bessonov, Zh. Tekh. Fiz. **42**, 1921 (1972) [Sov. Phys.Tech. Phys. **17**, 1540 (1973)].
[16]D. F. Alferov, Yu. A. Bashmakov, K. A. Belovintsev, *et al.*, in *Proc. of the Third All-Union Conf. on Charged-Particle Accelerators* (in Russian), Nauka, M., 1973, Vol. 1, p. 39.
[17]D. F. Alferov, Yu. A. Bashmakov, and E. G. Bessonov, Trudy FIAN SSSR 80, 100 (1975) [Proc. (Tr.) P. N. Lebedev Phys. Inst. Acad. Sci. USSR **80** (1975)].
[18]D. F. Alferov, Yu. A. Bashmakov, K. A. Belovintsev, E. G. Bessonov, and P. A. Cherenkov, Part. Acceler. **9**, 223 (1979).
[19]I. M. Ternov, V. R. Khalilov, V. G. Bagrov, and M. M. Nikitin, Izv. Vyssh. Uchebn. Zaved. Fiz. No. 2, 5 (1980) [Sov. Phys. J. **23**, 79 (1980)].
[20]N. A. Korkhmazian, Rad. Eff. **56**, 33 (1981).
[21]V. N. Baĭer, V. M. Katkov, and V. M. Strakhovenko, Zh. Eksp. Teor. Fiz. **80**, 1348 (1981) [Sov. Phys. JETP **53**, 688 (1981)].
[22]D. F. Alferov, Yu. A. Bashmakov, K. A. Belovintsev, E. G. Bessonov, and P. A. Cherenkov, Pis'ma Zh. Eksp. Teor. Fiz. **26**, 525 (1977) [JETP Lett. **26**, 385 (1977)].
[23]D. F. Alferov, Yu. A. Bashmakov, K. A. Belovintsev, E. G. Bessonov, and P. A. Cherenkov, Usp. Fiz. Nauk **128**, 177 (1979) [Sov. Phys. Usp. **22**, 381 (1979)].
[24]D. F. Alferov, Yu. A. Bashmakov, and P. A. Cherenkov, Dokl. Akad. Nauk SSSR **251**, 1106 (1980) [Sov. Phys. Dokl. **25**, 276 (1980)].
[25]D. F. Alferov, Yu. A. Bashmakov, A. S. Lerman, A. N. Livshits, V. V. Mikhaĭlin, and P. A. Cherenkov, Dokl. Akad. Nauk SSSR **256**, 574 (1981) [Sov. Phys. Dokl. **26**, 72 (1981)].
[26]D. F. Alferov, Yu. A. Bashmakov, and P. A. Cherenkov, Rad. Eff. **56**, 47 (1981).
[27]A. N. Didenko, A. V. Kozhevnikov, A. F. Medvedev, and M. M. Nikitin, Pis'ma Zh. Tekh. Fiz. **4**, 699 (1978) [Sov. Tech. Phys. Lett. **4**, 281 (1978)].
[28]A. N. Didenko, A. V. Kozhevnikov, A. F. Medvedev, M. M. Nikitin, and V. Ya. Épp, Zh. Eksp. Teor. Fiz. **76**, 1919 (1979) [Sov. Phys. JETP **49**, 973 (1979)].
[29]M. M. Nikitin, A. F. Medvedev, M. B. Moiseev, *et al.*, Zh. Tekh. Fiz. **51**, 584, 592 (1981) [Sov. Phys. Tech. Phys. **26**, 350, 355 (1981)].
[30]N. A. Vinokurov, E. S. Gluskin, G. A. Korniukhin, V. A. Kochubei, G. N. Kulipanov, N. A. Mezentsev, V. F. Pindiurin, A. N. Skrinsky, and V. M. Khorev, Nucl. Instr. and Meth. **177**, 239 (1980).
[31]H. Winick, G. Brown, K. Halbach, and J. Harris, Phys. Today **34**, No. 5, 50 (1981).
[32]H. Winick, R. Boyce, G. Brown, *et al.*, Nucl. Instr. and Meth. **208**, 127 (1983).
[33]R. Barbini, G. Vignola, S. Trillo, *et al.*, Preprint, presented to the Colloque Intern. sur les Laser a Electrons Libres. Bendor, France, Sept. 26–Oct. 1, 1982.
[34]Y. Farge, Appl. Opt. **19**, 4021 (1980).
[35]M. Billardon, D. A. G. Deacon, P. Elleaume, *et al.*, J. Phys. (Paris) **44**, C1-29 (1983).
[36]H. Maezawa, S. Mitani, K. Suzuki, *et al.*, Nucl. Instr. and Meth. **208**, 151 (1983).
[37]H. Maezawa, Y. Suzuki, H. Kitamura, *et al.*, Appl. Opt. **25**, 3260 (1986).
[38]P. Gürtler, Nucl. Instr. and Meth. A **246**, 91 (1986).
[39]D. A. G. Deacon, L. R. Elias, J. M. M. Madey, *et al.*, Phys. Rev. Lett. **38**, 892 (1977).
[40]S. Benson, D. A. G. Deacon, J. N. Eckstein, *et al.*, Phys. Rev. Lett. **48**, 235 (1982).
[41]C. Pellegrini, IEEE Trans. Nucl. Sci. **NS-26**, 3791 (1979).
[42]H. Motz, Contemp. Phys. **20**, 547 (1979).
[43]V. L. Bratman, N. S. Ginzburg, and M. I. Petelin, Zh. Eksp. Teor. Fiz. **76**, 930 (1979) [Sov. Phys. JETP **49**, 469 (1979)].
[44]L. A. Vaĭnshteĭn, Zh. Tekh. Fiz. **49**, 1129 (1979) [Sov. Phys. Tech. Phys. **24**, 625 (1979).
[45]A. A. Varfolomeev, Free Electron Lasers and Prospects of their Development (in Russian), Institute of Atomic Energy, M., 1980.
[46]M. V.Fedorov, Usp. Fiz. Nauk **135**, 213 (1981) [Sov. Phys. Usp. **24**, 801 (1981)].
[47]A. N. Didenko and A. V. Kozhevnikov, Vyssh. Uchebn. Zaved. Fiz. No. 3, 12 (1983) [Sov. Phys. J. **26**, 219 (1983)].
[48]D. F. Alferov, Yu. A. Bashmakov, K. A. Belovintsev, E. G. Bessonov, A. V. Serov, and P. A. Cherenkov, Zh. Tekh. Fiz. **53**, 270 (1983) [Sov. Phys. Tech. Phys. **28**, 167 (1983)].
[49]Generators of coherent radiation in free electron lasers (in Russian), a collection of articles, translated from English, edited by A. A. Rukhadze, Mir, M., 1983.
[50]A. N. Lebedev, Priroda, No. 9, 28 (1984).
[51]P. Sprangle and T. Coffey, Phys. Today **37**(3), 44 (1984) [Russ. transl., Usp. Fiz Nauk **146**, 303 (1985)].
[52]L. D. Landau and E. M. Lifshitz, *The Classical Theory of Fields*, 3rd ed., Pergamon Press, Oxford, 1971 [Russ. original, Nauka, M., 1967].
[53]V. L. Ginzburg, *Theoretical Physics and Astrophysics*, Pergamon Press, Oxford, 1979 [Russ. original, Nauka, M., 1975].
[54]J. D. Jackson, *Classical Electrodynamics*, Wiley, N.Y., 1962 [Russ. transl. Mir, M., 1965].
[55]D. F. Alferov, Yu. A. Bashmakov, and E. G. Bessonov, Kratk. Soobshch. Fiz. FIAN SSSR, No. 8, 47 (1972) [Sov. Phys. Lebedev Inst. Rep. (1972)].
[56]N. A. Korkhmazyan, Izv. AN ArmSSR. Ser. Fizika 7, 114 (1972).
[57]D. F. Alferov, Yu. A. Bashmakov, and E. G. Bessonov, Zh. Tekh. Fiz. **43**, 2126 (1973) [Sov. Phys. Tech. Phys. **18**, 336 (1974)].
[58]G. A. Schott, Electromagnetic Radiation, Cambridge Univ. Press, 1912.
[59]A. N. Matveev, Vestn. Mosk. Un-ta, Ser. Fizika, astronomiya, No. 10, 33 (1951).
[60]N. A. Korkhmazyan, Izv. ArmSSR, Ser. Fizika **5**, 287 (1970).

[61]E. S. Sarachik and G. T. Schappert, Phys. Rev. D **1**, 2738 (1970).
[62]R. Combe and M. Feix, C. R. Ac. Sci., Paris, **237**, 1318 (1953) [Russ. transl. Ref. 12, p. 340].
[63]Yu. A. Baschmakov and E. G. Bessonov, Rad. Eff. **66**, 85 (1982).
[64]D. F. Alferov, Yu. A. Bashmakov, and E. G. Bessonov, Preprint FIAN SSSR, No. 23, M., 1972.
[65]B. Levush, T. M. Antonsen, and W. M. Manheimer, J. Appl. Phys. **60**, 1584 (1986).
[66]D. F. Zaretskiĭ, É. A. Nersesov, K. B. Oganesyan, and V. M. Fedorov, Kvantovaya Elektron. (Moscow) **13**, 685 (1986) [Sov. J. Quantum Electron. **16**, 448 (1986)].
[67]A. P. Banford, *The Transport of Charged Particle Beams*, Spon, London, 1966 [Russ. transl., Atomizdat, M., 1969].
[68]J. Lindhard, Influence of Crystal Lattice on Motion of Energetic Charged Particles, Mat. Fys. Medd. Dan. Vid. Selsk. **34**, No. 14 (1965) [Russ. transl. Usp. Fiz. Nauk **99**, 249 (1969)].
[69]M. A. Kumakhov, Dokl. Akad. Nauk SSSR **230**, 1077 (1976) [Sov. Phys. Dokl. **21**, 581 (1976)].
[70]A. I. Akhiezer and N. F. Shul'ga, Usp. Fiz. Nauk **137**, 561 (1982) [Sov. Phys. Usp. **25**, 541 (1982)].
[71]V. A. Bazylev and N. K. Zhevago, Usp. Fiz. Nauk **137**, 605 (1982) [Sov. Phys. Usp. **25**, 565 (1982)].
[72]V. N. Baĭer, V. M. Katkov, and V. M. Strakhovenko, Dokl. Akad. Nauk SSSR **275**, 1369 (1984) [Sov. Phys. Dokl. **29**, 306 (1984)].
[73]V. G. Baryshevskiĭ, *Channeling, Radiation, and Reactions in Crystals at High Energies* (in Russian), Publishing House of the Belorussian University, Minsk, 1982.
[74]N. P. Kalashnikov, *Coherent Interactions of Charged Particles in a Single Crystal* (in Russian), Atomizdat, M., 1981.
[75]R. B. Palmer, J. Appl. Phys. **43**, 3014 (1972).
[76]J. Blewett and R. Chasman, J. Appl. Phys. **48**, 2692 (1977).
[77]J. H. Eberly, Progress in Optics, Ed. by E. Wolf, Amsterdam: North-Holland, 1967, Vol. 7, p. 359.
[78]V. N. Baĭer, V. M. Katkov, and V. M. Strakhovenko, Zh. Eksp. Teor. Fiz. **63**, 2121 (1972) [Sov. Phys. JETP **36**, 1120 (1973)].
[79]A. I. Nikishov and V. I. Ritus, Trudy FIAN SSSR **111**, 5, 152 (1979). [Proc. (Tr.) P. N. Lebedev Phys. Inst. Acad. Sci. USSR **111** (1979)].
[80]D. S. Gemmell, Rev. Mod. Phys. **46**, 129 (1974).
[81]A. A. Kolomenskiĭ and A. N. Lebedev, *Theory of Cyclic Accelerators*, Wiley, N.Y., 1966 [Russ. original, Fizmatgiz, M., 1962].
[82]V. N. Baĭer, V. M. Katkov, and V. M. Strakhovenko, Dokl. Akad. Nauk SSSR **246**, 1347 (1979) [Sov. Phys. Dokl. **24**, 469 (1979)].
[83]A. Hofmann, Nucl. Inst. and Meth. **151**, 17 (1978).
[84]R. Coisson, S. Guiducci, and M. A. Preger, Nucl. Instr. and Meth. **201**, 3 (1982).
[85]M. A. Ter-Mikaélyan, *Influence of the Medium on Electromagnetic Processes at High Energies* (in Russian), Publishing House of the Armenian Academy of Sciences, Erevan, 1969.
[86]Yu. G. Pavlenko, V. I. Petukhov, and A. Kh. Mussa, Izv. Vyssh. Uchebn. Zaved. Fiz. No. 10, 88 (1973) [Sov. Phys. J. **16**, 1411 (1973)].
[87]Yu. A. Bashmakov, Author's Abstract of Candidate's Dissertation, FIAN SSSR, M., 1979.
[88]D. F. Alferov, Yu. A. Bashmakov, and E. G. Bessonov, Proc. of the Sixth All-Union Conf. on Charged-Particle Accelerators (in Russian), JINR, Dubna, 1978, published at Dubna, 1979, Vol. 2, p. 216.
[89]M. B. Moiseev, M. M. Nikitin, and V. Ya. Épp, Izv. Vyssh. Uchebn. Zaved. Fiz. No. 9, 95 (1981) [Sov. Phys. J. **24**, 870 (1981)].
[90]A. Kh. Mussa, Yu. G. Pavlenko, and V. N. Petukhov, Vestn. Mosk. un-ta, Ser. Fizika, astronomiya, No. 3, 335 (1974).
[91]D. F. Alferov, Yu. A. Bashmakov, and E. G. Bessonov, Zh. Tekh. Fiz. **46**, 2392 (1976) [Sov. Phys. Tech. Phys. **21**, 1408 (1976)].
[92]B. Kincaid, J. Appl. Phys. **48**, 2684 (1977).
[93]D. F. Alferov, Yu. A. Bashmakov, E. G. Bessonov, and B. B. Govorkov Yad. Fiz. **27**, 971 (1978) [Sov. J. Nucl. Phys. **27**, 514 (1978)]; Trudy FIAN SSSR **147**, 27 (1983) [Proc. (Tr.) P. N. Lebedev Phys. Inst. Acad. Sci. USSR **147** (1983)].
[94]European Synchrotron Radiation Facility. Supplement II, The Machine, Ed. by D. Y. Thompson and M. W. Poole, Strasbourg, ESF, 1979.
[95]S. Krinsky, IEEE Trans. Nucl. Sci. **NS-30**, 3078 (1983).
[96]D. F. Alferov and Yu. A. Bashmakov, Zh. Tekh. Fiz. **55**, 829, 1090 (1985) [Sov. Phys. Tech. Phys. **30**, 497, 622 (1985)].
[97]D. F. Alferov and Yu. A. Bashmakov, Proc. of the Seventh All-Union Conf. on Charged-Particle Accelerators (in Russian), JINR, Dubna, 1981, Vol. 2, p. 130.
[98]M. W. Poole and R. P. Walker, Nucl. Instr. and Meth. **176**, 487 (1980).
[99]E. G. Bessonov, Zh. Tekh. Fiz. **56**, 2361 (1986) [Sov. Phys. Tech. Phys. **31**, 1413 (1986)].
[100]D. F. Alferov, Yu. A. Bashmakov, and E. G. Bessonov, Zh. Tekh. Fiz. **48**, 1592, 1598 (1978) [Sov. Phys. Tech. Phys. **23**, 902, 905 (1978)].
[101]Submillimeter Wave Technique (in Russian), Ed. by P. A. Valitov, Sov. Radio, M., 1969.
[102]A. N. Oraevskiĭ, Kvantovaya Elektron. (Moscow) **7**, 495 (1980) [Sov. J. Quantum Electron. **10**, 282 (1980)].
[103]N. A. Korkhmazyan, L. A. Gevorgyan, and M. P. Petrosyan, Zh. Tekh. Fiz. **47**, 1583 (1977) [Sov. Phys. Tech. Phys. **22**, 917 (1977)].
[104]D. F. Alferov, Yu. A. Bashmakov, and E. G. Bessonov, Preprint No. 234, FIAN SSSR, M., 1978.
[105]A. A. Kolomenskiĭ and A. N. Lebedev, Kvantovaya Elektron. (Moscow) **5**, 1543 (1978) [Sov. J. Quantum Electron. **8**, 879 (1978)].
[106]J. M. J. Madey, J. Appl. Phys. **42**, 1906 (1971).
[107]J. M. J. Madey, Nuovo Cimento, Ser. B **50**, 64 (1979).
[108]E. G. Bessonov, Preprint No. 289, FIAN SSSR, M., 1983.
[109]A. Einstein, Collected Scientific Works, Nauka, M., 1966, Vol. 3, p. 386.
[110]D. F. Alferov and Yu. A. Bashmakov, Kvantovaya Elektron (Moscow) **12**, 1926 (1985) [Sov. J. Quantum Electron. **15**, 1271 (1985)].
[111]V. N. Bair and A. I. Milstein, Phys. Lett. **65A**, 319 (1978).
[112]D. F. Alferov and E. G. Bessonov, Zh. Tekh. Fiz. **49**, 777 (1979) [Sov. Phys. Tech. Phys. **24**, 450 (1979)].
[113]E. G. Bessonov and A. V. Serov, Zh. Tekh. Fiz. **52**, 383 (1982) [Sov. Phys. Tech. Phys. **27**, 245 (1982)].
[114]A. M. Kondratenko and E. L. Saldin, Dokl. Akad. Nauk SSSR **249**, 843 (1979) [Sov. Phys. Dokl. **24**, 986 (1979)].
[115]Y. W. Chan, Phys. Lett. **76A**, 25 (1980).
[116]N. A. Vinokurov and A. N. Skrinskiĭ, Preprint No. 77-59, Institute of Nuclear Physics, Siberian Division, USSR Academy of Sciences, Novosibirsk, 1977.
[117]W. B. Colson and R. A. Freedman, Phys. Rev. A **27**, 1399 (1983).
[118]L. R. Elias, Phys. Rev. Lett. **16**, 977 (1979).
[119]C. Pellegrini, Nucl. Instr. and Meth. **177**, 227 (1980).
[120]D. A. Deacon, Nucl. Instr. and Meth. **208**, 171 (1983).
[121]V. N. Korchuganov, G. N. Kulipanov, N. A. Mezentsev, A. N. Skrinsky, and N. A. Vinokurov, Nucl. Instr. and Meth. **208**, 11 (1983).
[122]A. Hofmann, Phys. Rep. **64**, 253 (1980).
[123]D. F. Alferov, Author's Abstract of Candidate's Dissertation, FIAN SSSR, 1979.
[124]M. W. Poole and R. P. Walker, Preprint DL/SCI/P283A, Daresbury, 1981.
[125]K. Halbach, Nucl. Instr. and Meth. **169**, 1 (1980).
[126]G. Brown, H. Winick, and P. Eisenberger, Nucl. Instr. and Meth. **204**, 543 (1983).
[127]M. W. Fan. M. W. Poole, and R. P. Walker, Preprint DL/SCI/TM30A, Daresbury, 1981.
[128]V. L. Bratman, G. M. Genkin, and V. V. Zil'berberg, Pis'ma Zh. Tekh. Fiz. **8**, 970 (1982) [Sov. Tech. Phys. Lett. **8**, 419 (1982)].
[129]V. I. Alekseev, D. F. Alferov, Yu. A. Bashmakov *et al.*, Preprint No. 186, FIAN SSSR, M., 1983.
[130]E. G. Bessonov, Preprint No. 18, FIAN SSSR, M., 1982.
[131]A. F. Medvedev and M. M. Nikitin, Izv. Vyssh. Uchebn. Zaved. Fiz., No. 9, 87 (1978) [Sov. Phys. J. **21**, 1182 (1978)].
[132]R. Coisson, Nucl. Instr. and Meth. **108**, 185 (1983).
[133]W. M. Grossman, J. M. Slater, D. C. Quimby, *et al.*, Appl. Phys. Lett. **43**, 745 (1983).
[134]K. Boyer, C. A. Brau, B. E. Newman *et al.*, IEEE Trans. Nucl. Sci. **NS-30**, 3076 (1983).
[135]J. A. Edighoffer, G. R. Neil, C. E. Hess *et al.*, Phys. Rev. Lett. **52**, 344 (1984).
[136]V. L. Granatstein, W. W. Destler, and I. O. Mayergoyz, Appl. Phys. Lett. **47**, 643 (1985).
[137]E. S. Gluzskin *et al.*, Preprint No. 83-145, Institute of Nuclear Physics, Siberian Division, USSR Academy of Sciences, Novosibirsk, 1983.
[138]M. Billardon, P. Elleaume, J. M. Ortega *et al.*, Phys. Rev. Lett. **51**, 1652 (1983).
[139]N. A. Vinokurov and A. N. Skrinskiĭ, *Relativistic High Frequency Electronics* (in Russian), Ed. by A. V. Gaponov-Grekhov, Gorkiĭ, Institute of Applied Physics, USSR Academy of Sciences, 1981, p. 204.
[140]M. M. Nikitin, A. F. Medvedev, M. B. Moiseev, and V. Ya. Épp, Zh. Eksp. Teor. Fiz. **79**, 763 (1980) [Sov. Phys. JETP **52**, 388 (1980)].
[141]D. F. Alferov and Yu. A. Bashmakov, Pis'ma Zh. Eksp. Teor. Fiz. **34**, 15 (1981) [JETP Lett. **34**, 13 (1981)].
[142]C. L. Artem'ev, E. M. Moroz, V. A. Orlov *et al.*, Kratk. Soobshch. Fiz., FIAN SSSR, No. 11, 58 (1981) [Sov. Phys. Lebedev Inst. Rep. (1981)].
[143]E. G. Bessonov, Zh. Tekh. Fiz. **53**, 1368 (1983) [Sov. Phys. Tech. Phys. **28**, 837 (1983)].
[144]Yu. A. Bashmakov, Zh. Tekh. Fiz. **56**, 515 (1986) [Sov. Phys. Tech. Phys. **31**, 310 (1986)].
[145]Yu. A. Bashmakov, V. S. Karpov, and A. S. Yarov, Zh. Tekh. Fiz. **54**, 905 (1984) [Sov. Phys. Tech. Phys. **29**, 539 (1984)].

[146]A F. Medvedev, M. M. Nikitin, and V. Ya. Épp, Pis'ma Zh. Tekh. Fiz. **5**, 359 (1979) [Sov. Tech. Phys. Lett. **5**, 144 (1979)].
[147]A. Maitland and M. H. Dunn, Laser Physics, North-Holland, Amsterdam, 1969 [Russ. transl., Nauka, M., 1978].
[148]A F. Medvedev, M. M. Nikitin, and V. Ya. Épp, Pis'ma Zh. Tekh. Fiz. **5**, 795 (1979) [Sov. Tech. Phys. Lett. **5**, 327 (1979)].
[149]E. S. Gluskin, S. N. Gaponov, S. A. Gusev *et al.*, Preprint No. 83-163, Institute of Nuclear Physics, Siberian Division, USSR Academy of Sciences, Novosibirsk, 1983.
[150]I. I. Miroshnichenko, J. J. Murray, R. O. Avakyan, and T. Kh. Figut, Pis'ma Zh. Eksp. Teor. Fiz. **29**, 786 (1979) [JETP Lett. **29**, 722 (1979)].
[151]R. O. Avakyan, I. I. Miroshnichenko, J. J. Murray, and T. Figut, Zh. Eksp. Teor. Fiz. **82**, 1825 (1982) [Sov. Phys. JETP **55**, 1052 (1982)].
[152]H. Bochmer, M. Z. Caponi, J. Edighoffer *et al.*, Phys. Rev. Lett. **48**, 141 (1982).
[153]L. R. Elias, J. Hu, and G. Ramian, Nucl. Instr. and Meth. Ser. A **237**, 203 (1985).
[154]D. F. Alferov and E. G. Bessonov, Pis'ma Zh. Tekh. Fiz. **3**, 828 (1977) [Sov. Tech. Phys. Lett. **3**, 336 (1977)].
[155]R. Coisson, Nucl. Instr. and Meth. **143**, 241 (1977).
[156]J. Bosser, L. Burnod, R. Coisson *et al.*, IEEE Trans. Nucl. Sci. **NS-30**, 2164 (1983).
[157]V. V. Anashin, V. B. Baryshev, N. A. Vinokurov *et al.*, Papers at the All-Union Conf. on Use of Synchrotron Radiation SR-82 (in Russian), Novosibirsk, 1982, p. 3.
[158]E. Umbach, SSRL Report 192, P. VII–131.
[159]A. N. Skrinskiĭ, Usp. Fiz. Nauk **138**, 3 (1982) [Sov. Phys. Usp. **25**, 639 (1982)].
[160]V. E. Balakin and A. A. Mikhaĭlenko, Proc. of the Seventh All Union Conf. on Charged-Particle Accelerators (in Russian), JINR, Dubna, 1981, Vol. 2, p. 302.
[161]Yu. A. Bashmakov and E. G. Bessonov, Proc. of the Tenth Int. Conf. on High Energy Charged-Particle Accelerators (in Russian), Serpukhov, 1977, Vol. 2, p. 118.
[162]G. Ya. Kezerashvili, A. P. Lysenko, V. M. Khorev, G. M. Chernykh, and Yu. M. Shatunov, Papers at the All-Union Conf. on Use of Synchrotron Radiation SR-82 (in Russian), Novosibirsk, 1982, p. 109.
[163]N. A. Vinokurov, Nucl. Instr. and Meth., Ser. A **246**, 105 (1986).

Translated by Clark S. Robinson